

AD-A020 127

INVESTIGATION OF INTERNAL CORROSION AND EVALUATION OF  
NON-SKID COATINGS ON MARK 7 JET BLAST DEFLECTORS

George A. Gehring, Jr.

Naval Air Engineering Center  
Lakehurst, New Jersey

10 December 1975

DISTRIBUTED BY:

**NTIS**

National Technical Information Service  
U. S. DEPARTMENT OF COMMERCE

**NAVAL AIR ENGINEERING CENTER**  
**LAKEHURST, NEW JERSEY 08733**

**ENGINEERING DEPARTMENT (SI)**  
**CODE IDENT. NO. 80020**

**NAEC-ENG-7875**

**10 Dec 1975**

**INVESTIGATION OF INTERNAL CORROSION  
AND EVALUATION OF NON-SKID COATINGS ON  
MARK 7 JET BLAST DEFLECTORS**

**PREPARED BY** George A. Gehring, Jr.

**GEORGE A. GEHRING, JR.**

**APPROVED BY** 10A [Signature]

i.

PLATE NO. 20000

10 DEC 1975 BH

Unclassified

SECURITY CLASSIFICATION OF THIS PAGE (When Data Entered)

REPORT DOCUMENTATION PAGE		READ INSTRUCTIONS BEFORE COMPLETING FORM									
1. REPORT NUMBER <b>NAEC-ENG-7875</b>	2. GOVT ACCESSION NO.	3. RECIPIENT'S CATALOG NUMBER									
4. TITLE (and Subtitle) <b>Investigation of Internal Corrosion and Evaluation of Non-Skid Coatings on Mark 7 Jet Blast Deflectors</b>		5. TYPE OF REPORT & PERIOD COVERED <b>Final</b>									
		6. PERFORMING ORG. REPORT NUMBER									
7. AUTHOR(s) <b>George A. Gehring, Jr.</b>		8. CONTRACT OR GRANT NUMBER(s) <b>N00156-73-C-0962</b>									
9. PERFORMING ORGANIZATION NAME AND ADDRESS <b>Naval Air Engineering Center Lakehurst, NJ 08733</b>		10. PROGRAM ELEMENT, PROJECT, TASK AREA & WORK UNIT NUMBERS									
11. CONTROLLING OFFICE NAME AND ADDRESS <b>Naval Air Systems Command Headquarters Washington, DC 20361 AIR-537</b>		12. REPORT DATE <b>10 Dec 1975</b>									
14. MONITORING AGENCY NAME & ADDRESS (if different from Controlling Office) <b>Naval Air Systems Command Headquarters Washington, DC 20361 AIR-537</b>		13. NUMBER OF PAGES <b>79</b>									
		15. SECURITY CLASS. (of this report) <b>Unclassified</b>									
16. DISTRIBUTION STATEMENT (of this Report) <b>Approved for public release; distribution unlimited</b>											
17. DISTRIBUTION STATEMENT (of the abstract entered in Block 20, if different from Report)											
18. SUPPLEMENTARY NOTES <b>COLOR ILLUSTRATIONS REPRODUCED IN BLACK AND WHITE</b>											
19. KEY WORDS (Continue on reverse side if necessary and identify by block number) <table><tr><td>Corrosion</td><td>Sea Water</td><td>Flight Deck Environment</td></tr><tr><td>Coatings</td><td>Non-Skid</td><td>Abrasion Resistance</td></tr><tr><td>Simulated Test</td><td>Jet Blast Deflectors</td><td>Metal Spray</td></tr></table>			Corrosion	Sea Water	Flight Deck Environment	Coatings	Non-Skid	Abrasion Resistance	Simulated Test	Jet Blast Deflectors	Metal Spray
Corrosion	Sea Water	Flight Deck Environment									
Coatings	Non-Skid	Abrasion Resistance									
Simulated Test	Jet Blast Deflectors	Metal Spray									
20. ABSTRACT (Continue on reverse side if necessary and identify by block number) <p>The Mark 7 Jet Blast Deflector (JBD) is a 36 foot by 14 foot aluminum barrier erected at a 50 degree angle to the flight deck, for the purpose of protecting waiting aircraft and handling personnel from the jet blast of a plane being launched. In order to cool the panels enough to allow safe passage of personnel and machinery and to prevent actual physical damage to the JBD by the heat of the jet engines, sea water is pumped through</p>											

the internal passages of the panels. Ships personnel, in the past, have reported that internal corrosion was a continuing maintenance problem, requiring frequent and costly rework. In line with the Navy's goal of reducing ship maintenance costs and improving hardware reliability, NAVAIRENGCEN undertook a program to assess the severity of corrosion damage occurring on the JBD's and investigate potential methods for controlling internal corrosion. NAVAIRENGCEN also initiated a study to further evaluate the relative ability of metallic non-skid coatings to perform in the JBD carrier deck environment. The entire program was conducted in a natural sea water environment at Ocean City, NJ to insure realistic simulation of the carrier deck environment. This report presents the results of the program.

ib

## I. INTRODUCTION

The Mark 7 Jet Blast Deflector (JBD) is a 36 foot by 14 foot aluminum barrier erected at a 50 degree angle to the flight deck, for the purpose of protecting waiting aircraft and handling personnel from the jet blast of a plane being launched. In order to cool the panels enough to allow safe passage of personnel and machinery and to prevent actual physical damage to the JBD by the heat of the jet engines, sea water is pumped through the internal passages of the panels. Ships personnel, in the past, have reported that internal corrosion was a continuing maintenance problem, requiring frequent and costly rework. In line with the Navy's goal of reducing ship maintenance costs and improving hardware reliability, NAVAIRENGCEN undertook a program to assess the severity of corrosion damage occurring on the JBD's and investigate potential methods for controlling internal corrosion. NAVAIRENGCEN also initiated a study to further evaluate the relative ability of metallic non-skid coatings to perform in the JBD carrier deck environment. The entire program was conducted in a natural sea water environment at Ocean City, NJ to insure realistic simulation of the carrier deck environment. This report presents the results of the program.

## II. SUMMARY

The program determined that copper present in the sea water cooling supply is the primary cause of internal corrosion of the JBD's. The copper originates from copper-nickel fire water mains located upstream of the JBD's. If copper is continually present in the cooling water at the concentrations measured in this program, then it is estimated that the Mark 7 modules will have a useful service life of from two to four years. If copper were not present in the cooling water, the service life would exceed 20 years. The program failed to determine a practical method for removing the copper or a coating which could be effectively used to reduce internal corrosion. Tests are underway to establish the practical level of copper in operational systems and will be used as the basis for further evaluation.

The program also rated several metal-spray non-skid deck coatings on their stability in a simulated flight deck environment when applied over an aluminum substrate. The coatings which exhibited the best resistance to this harsh environment include arc-sprayed aluminum, arc-sprayed aluminum molybdenum, and arc-sprayed aluminum titanium. Flame-sprayed nickel-aluminide exhibited the best abrasion resistance. Determination of the optimum non-skid coating depends on the results of in-service performance tests now in progress on different aircraft carriers; future efforts will be based on these tests.

## III. TABLE OF CONTENTS

<u>SUBJECT</u>	<u>PAGE</u>
I. INTRODUCTION . . . . .	i
II. SUMMARY . . . . .	i
III. TABLE OF CONTENTS . . . . .	ii
IV. LIST OF TABLES AND FIGURES . . . . .	iii
V. INVESTIGATION OF INTERNAL CORROSION AND EVALUATION OF NON-SKID COATINGS ON MARK 7 JET BLAST DEFLECTORS . . . . .	1
A. Introduction . . . . .	1
B. Investigation of Internal Corrosion and Methods for Controlling Internal Cor- rosion . . . . .	2
1. Experimental Procedures . . . . .	2
2. Results . . . . .	7
3. Conclusions . . . . .	14
4. Future Actions . . . . .	15
C. Evaluation of Non-Skid Deck Coatings . . . . .	15
1. Experimental Procedures . . . . .	15
2. Results . . . . .	17
3. Conclusions . . . . .	19
4. Future Actions . . . . .	20
VI. TABLES AND FIGURES . . . . .	21
Appendix 1 - The Use of Electrochemical Polarization Techniques to Measure Corrosion Rates. . . . .	62-64
Appendix 2 - Evaluation of Protective Coatings by Electrochemical Potential and Polarization Measurements. . . . .	65-66
Appendix 3 - Fleet Evaluations of Various Non-Skid Coatings Applied to Jet Blast Deflectors. . . . .	67-70

## IV. LIST OF TABLES AND FIGURES

	<u>Title</u>	<u>Page</u>
Table I	- JBD Cooling Water Analysis For Iron and Copper . . . . .	21
Table II	- Local Action Corrosion Rates and Potentials for Weld Test Specimens.	22
Table III	- Candidate Coatings for Use on the Internal Surfaces of the JBD . . .	23
Table IV	- General Corrosion Rates For Coated 6061-T6 Aluminum Test Coupons in Sea Water @ 100°C . . . . .	24
Table V	- Initial Corrosion Rate Data For JBD Test Loop . . . . .	25
Table VI	- Periodic Corrosion Rate Data For JBD Test Loop (Run No. 1) . . . . .	26
Table VII	- Periodic Corrosion Rate Data For JBD Test Loop (Run No. 2) . . . . .	27
Table VIII	- Periodic Corrosion Rate Data For JBD Test Loop (Run No. 3) . . . . .	28
Table IX	- Candidate Non-Skid Coatings Selected For Testing . . . . .	29
Table X	- General Description of Metal-Spray Coating Performance . . . . .	33
Table XI	- Periodic Corrosion Rates (MPY) For Metal-Spray Exposure Panels . . . . .	36
Table XII	- Periodic Corrosion Potentials For Metal Spray Exposure Panels . . . . .	39
Figure 1	- F-14 at Mark 7 Jet Blast Deflector.	42
Figure 2	- 2' x 6' Aluminum Module Section Used to Assemble JBD . . . . .	43
Figure 3	- Test Specimen Used in Screening Tests for Internal Coatings . . . . .	44
Figure 4	- Test Loop for Simulating Internal Corrosion of the JBD's . . . . .	45

	<u>Page</u>
Figure 5 - Arrangement for Heating Test Module Section . . . . .	46
Figure 6 - Internal Corrosion Attack on Mark 6 JBD Panel Removed From USS Kitty Hawk . . . . .	47
Figure 7 - Internal Corrosion Attack on Mark 6 JBD Panel Removed From USS Kitty Hawk . . . . .	47
Figure 8 - Internal Corrosion Attack on Mark 6 JBD Panel Removed From USS Kitty Hawk . . . . .	48
Figure 9 - Internal Corrosion Attack on Mark 6 JBD Panel Removed From USS Kitty Hawk . . . . .	48
Figure 10 - Corrosion Attack on Inlet Pipe on Mark 6 JBD Panel Removed From USS Kitty Hawk . . . . .	49
Figure 11 - Simplified Schematic of JBD Test Loop . . . . .	50
Figure 12 - Internal Surface of Test Section After 3-Months Exposure Test (No copper injection) . . . . .	51
Figure 13 - Internal Surface of Test Section After 3-Months Exposure Test (3 ppm copper injection) . . . . .	51
Figure 14 - Internal Surface of Coated Test Section After 3-Months Exposure Test (3 ppm copper injection) . . . . .	52
Figure 15 - Test Set-Up for Making Polarization Measurements . . . . .	53
Figure 16 - Test Rig Built to Evaluate Non-Skid Deck Coatings . . . . .	54
Figure 17 - Close-Up of Test Rig Built to Evaluate Non-Skid Deck Coatings . . . . .	55
Figure 18 - Set-Up For Abrasion Resistance Tests . . . . .	56
Figure 19 - Nickel-Aluminide Coating (<15 mils) After 5-Month Exposure . . . . .	57



	<u>Page</u>
Figure 20 - Nickel-Aluminide Coating (>15 mils) After 1-Month Exposure . . . . .	58
Figure 21 - Nickel-Aluminide Coating (>15 mils) After 1-Month Exposure . . . . .	58
Figure 22 - Wire-Spray Aluminum Coating After 1-Month Exposure . . . . .	59
Figure 23 - Alumina-Titania Coating After 9- Months Exposure . . . . .	60
Figure 24 - Comparison of Abrasion Resistance For Candidate Non-Skid Coatings . .	61

V. INVESTIGATION OF INTERNAL CORROSION AND EVALUATION OF  
NON-SKID COATINGS ON MARK 7 JET BLAST DEFLECTORS

A. INTRODUCTION. The Mark 7 Jet Blast Deflector (JBD) is a 36 foot by 14 foot aluminum barrier used to protect waiting aircraft from direct impingement of jet exhaust from the aircraft being launched. Deck handlers and personnel servicing the awaiting aircraft must also be protected from jet blasts and FOD (foreign objects on deck) hurled by the jet stream. A JBD is located just aft of each catapult and is stowed flush with the flight deck. After the aircraft taxis into launch position the JBD is raised to a 50 degree angle so that the engine exhaust impinges on the forward face of the barrier and is deflected upward. Figure 1 shows the general arrangement.

The extreme heat generated by the jet engine would make passage of personnel and machinery over a lowered JBD impossible and would ultimately render the JBD useless due to damage caused by the heat. In order to eliminate the above problems, cooling is required.

The Mark 7 JBD is a relatively new design developed by NAVAIRENGCEN to provide increased cooling capacity required for launching larger aircraft such as the F 14. The Mark 7 design incorporates modular construction. An array of 42 individual 2' x 6' aluminum modules are manifolded together. Thus, if replacement is required, a single 2' x 6' panel can be removed rather than a much larger section as was required with the former design (Mark 6). The modules are extruded from 6061-T6 aluminum plate. Figure 2 shows a single module.

In the past, ship's personnel reported that internal corrosion was a major and continuing maintenance problem on the Mark 6 panels, requiring frequent and costly rework. Quite frequently, replacements for the old, larger sections were not available. Pieces of aluminum hardware (e.g. inlet pipe elbows) periodically returned to NAVAIRENGCEN for inspection showed significant internal corrosion.

The service environment which the JBD's must withstand is extremely corrosive. The typical environment to which the external surfaces of the JBD are subjected includes:

1. Heat (jet blast approaching 1000°C, skin temperature about 200°C)
2. Sea water spray and washdown

3. JP-5 jet fuel-detergent washdown
4. Aircraft cleaning solution
5. Lube Oil
6. Hydraulic Fluid
7. Marine Atmosphere
8. Impact
9. Abrasion
10. SO<sub>2</sub> from stack gases

The internal surfaces of the JBD are subjected to flowing sea water at temperatures approaching 100°C.

In line with the Navy's goal of reducing ship maintenance costs and improving hardware reliability, NAVAIRENGCEN undertook a program to assess the severity of corrosion damage occurring in the JBD's and investigate potential methods for controlling internal corrosion. Since, in the stowed position, the JBD becomes a portion of the flight deck, it is necessary that a non-skid type coating be applied to the external surface. To date, the normal flight deck epoxy non-skid has been ineffective in withstanding the harsh environment outlined above. Previous investigation<sup>1</sup> of metallic non-skid coatings determined that several coatings exhibited favorable non-skid characteristics. However, the corrosion rates of some of the coatings were excessive. For this reason, NAVAIRENGCEN also initiated a study to further evaluate the relative ability of metallic non-skid coatings to perform in the JBD-carrier deck environment. This report presents the results of the test program.

## B. INVESTIGATION OF INTERNAL CORROSION AND METHODS FOR CONTROLLING INTERNAL CORROSION

### 1. EXPERIMENTAL PROCEDURES

a. JBD PANEL INSPECTION. JBD panels were removed from operational carriers and returned to NAVAIRENGCEN for inspection. The panels were cut open and inspected for pitting, scaling, and other forms of deterioration. Pit depths were measured and the frequency of pitting was noted. In addition, qualitative wet chemical tests were made to detect the presence of copper and iron at pits and in surface films.

<sup>1</sup>Dr. R. W. W. W. W., "Development of Metallized Non-Skid and Jet Blast Deflectors" NAEC Report No. 7849, August, 1974.

The qualitative chemical test for copper consisted of wetting the immediate area surrounding a pit with concentrated nitric acid and then absorbing the acid solution from the surface with a piece of filter paper. The filter paper was then exposed to ammonium hydroxide vapor. Theoretically, if copper is present on the metal surface, it should dissolve in the nitric acid. Exposure to ammonium hydroxide vapor will neutralize the acid and cause blue copper hydroxide to precipitate out.

The qualitative chemical test used to detect the presence of iron consisted of dissolving the surface film in hydrochloric acid and then adding a drop of 1N ammonium thiocyanate solution. If iron is present, the clear solution will turn pink to dark red depending on the concentration of iron.

b. COOLING WATER ANALYSES. Cooling water samples were obtained from three (3) operational carriers at different points in the JBD seawater supply system. The water samples were analyzed for iron and copper using colorimetric techniques. For copper, the Cuprethol Method was used. For iron, the Phenanthroline Method was used.

c. WELD SENSITIZATION TESTS. Both electron beam welding and arc welding are required during final fabrication of a JBD module. For the arc weld, 5456 aluminum alloy is used as the filler metal. Tests were conducted to determine if the weld areas were sensitized (more susceptible to localized corrosion).

Localized corrosion occurs at sensitized weld areas primarily because of galvanic differences that exist between the weld metal, heat-affected zone, and/or the base metal. The heat of welding can cause segregation or agglomeration of second phase precipitates within the microstructure of the alloy. The second phase precipitate often differs in electrochemical potential from the primary phase. This potential difference can give rise to local galvanic cells at welds and significantly increase corrosion susceptibility.

To investigate this phenomena, sections were cut from actual welds (both electron beam and arc) on production-line JBD modules. Test specimens were cut from the base metal, heat-affected zone, and weld metal. The test specimens were then immersed in sea water @ 100°C for 24 hours. The corrosion potential and corrosion rate of each test specimen were measured. Polarization resistance methods were used to determine the corrosion rate. Appendix I describes this technique.

In addition to electrochemical tests, an accelerated exposure test was also conducted to detect possible weld sensitization. The test consisted of exposing a test specimen cut from a production weld to the following solution:

Sodium Chloride - 57 grams

Hydrogen peroxide (30%) - 500 milliliters

Deionized water to make 1 liter.

The immersion period was 6 hours. All chemicals were reagent grade. At the end of the immersion period, the specimen was examined with a metallurgical microscope for evidence of localized corrosion.

#### d. SCREENING TESTS ON CANDIDATE INTERNAL COATINGS

(1) SELECTION. At the outset of the program, a literature search was initiated to identify candidate coatings that might be used to control internal corrosion of the JBD's. The choice of a protective coating applicable on the internal surfaces of the JBD is constrained by a number of factors. First, the JBD is a heat transfer device. Any coating applied internally to the JBD must be thermally conductive or provide minimal resistance to heat transfer.

In addition to possessing low thermal resistance, a candidate coating must be able to withstand the environment characteristic of the JBD. During a catapult shot, the external skin temperature of the JBD typically approaches 175°C to 200°C. The temperature gradient through the JBD skin is about 75°C. The sea water on exiting from the JBD is 100°C at a flow rate of 5 ft./sec. maximum. Any coating selected for testing must be resistant to sea water @ 100°C.

The last major constraint affecting the choice of coating is application. Because of the as-fabricated shape of the JBD modules (Figure 2), application of a protective coating to the internal surfaces of the finished product is difficult. The tight tolerances associated with the channel orificing demand that coating thickness be controllable with a good degree of accuracy.

(2) TESTING. All coatings identified as candidates for use on the internal surfaces of the JBD were screened for relative resistance to high temperature

sea water. Each coating was applied to a 1-inch dia. x 6-inch long piece of 6061-T6 aluminum bar. Figure 3 shows a typical test specimen. The coated test specimens were then immersed in sea water @ 100°C for a period of 30 days. Electrochemical polarization measurements were made during the exposure period. Appendix II describes the basis for these measurements. After completion of the exposure period, the coatings were visually inspected for deterioration.

#### e. SIMULATED EXPOSURE TESTS

(1) TEST LOOP DESIGN. In order to meaningfully investigate internal corrosion and methods for controlling internal corrosion, a test loop was constructed at Ocean City, New Jersey to provide a realistic simulation of the internal conditions characteristic of the JBD. The test loop arrangement is shown in Figure 4.

The test loop provided natural sea water at temperatures and flow velocities similar to those encountered in actual operation. The test loop utilized single channel sections cut from production-run panels. Each test section was 18 inches in length. In addition, 1-inch 6061-T6 aluminum pipe nipples were located upstream and downstream of the 18-inch sections. The pipe nipples were insulated from the 18-inch module sections and made possible the acquisition of electrochemical potential and polarization data. Also, 90° elbow sections (6061-T6 Al) inserted in each branch characterized the possible effects of turbulent water flow. The size of the 90° elbows was scaled to simulate water flow through manifold elbows on ship.

The test modules were arranged in parallel branches, two modules to a branch. The downstream modules in each branch afforded the capability of testing protective coatings. The upstream modules without protective coatings characterized corrosion as it occurs in actual shipboard service. Appropriate valving enabled individual flow control through each branch. Appropriate mixing tanks and metering pumps permitted simulation of heavy metal contamination.

Figure 5 shows the experimental set-up for providing the required heat to effect the desired aluminum skin temperatures. Five strip heaters (1000 watt) were mechanically fastened to a 1/2" copper plate along with the test module. The whole assembly was lagged with thermal insulation. The skin temperature of the module section was controlled by manually regulating power to the strip heaters. Temperatures were monitored by thermocouples.

All wetted materials in the test loop except for the test modules were non-metallic to avoid introduction of extraneous effects from contaminants. The materials were as follows:

Piping - chlorinated PVC, fiberglass

Valves - chlorinated PVC

Supply Tanks - Polyethylene

Pumps - PVC

Flowmeter - Borosilicate glass

Heat Exchanger - Teflon (R)

(2) TEST LOOP OPERATION. The flow through all test modules was cycled, simulating shipboard operation. The test cycle each day, Monday thru Friday was as follows:

(a) 8 hours, high temperature  
flowing sea water

(b) 16 hours, ambient temperature  
sea water, no flow

On weekends, the sea water was held at ambient temperatures with no flow through the module.

f. HEAVY METAL FILTER TESTS. Early in the program, it was determined that heavy metals (Fe, Cu) were present in the sea water supply systems onboard the aircraft carriers. It was later shown that heavy metal contamination (Cu) was significantly accelerating internal corrosion of the JBD. Therefore, screening tests were initiated to investigate the possibility of filtering out the heavy metals by using an active metal filter ahead of the modules. The tests comprised both beaker tests and simulated testing in the loop described previously.

For the beaker tests, different active metals (aluminum, zinc, and magnesium) were added at various concentrations to agitated sea water dosed with copper @ 3 ppm. The copper was added in the form of saturated copper sulphate solution. Pipet samples were extracted at various time intervals and measured for copper concentration. In this manner, a semi-quantitative estimate could be made of the quantity of each active metal required to filter or plate out the copper prior to entry into the JBD.

(R) Registered trademark of E.I. Dupont & Co.

In addition to the beaker tests, cartridge-type filters were made up of each active metal and installed in the test loop. Sea water dosed with copper at  $\approx 3$  ppm was pumped continuously through the loop on a once-thru basis. The water was sampled both upstream and downstream of the active metal filter.

## 2. RESULTS

### a. JBD PANEL INSPECTION

(1) MODULE RECEIVED FROM USS KITTY HAWK. Two JBD modules were returned from different aircraft carriers for inspection. The first panel was received from the USS Kitty Hawk (CVA-63). The panel was not of the new Mark 7 design but of the earlier Mark 6. The Mark 6 design differed from the Mark 7 in wall thickness and in the cross sectional dimensions of the internal flow channels. The Mark 6 modules have 10 parallel internal channels with cross sectional dimensions of  $\approx 1" \times 1 \frac{7}{16}"$ . The Mark 7 modules have 24 internal channels with cross sectional dimensions of  $\approx \frac{3}{4}" \times \frac{1}{4}"$ . The wall thickness of the Mark 6 module is  $\frac{5}{16}"$  on the topside and  $\approx \frac{5}{32}"$  on the underside. The Mark 7 wall thickness is uniform @  $\frac{1}{4}"$ .

The Mark 6 module returned from the Kitty Hawk had been in service for about 2 years and had seen about 9000 catapult shots. Initial inspection of the module showed seven (7) penetrations of the panel wall on the underside. No wall penetrations were found on the topside of the module. On sectioning the module, it was determined that the penetrations had resulted primarily from internal corrosion. However, significant corrosion had also occurred on the external underside of the module.

The pitting attack on the external underside of the JBD was highly localized in certain areas. The average depth of pitting in these areas was 40 mils with a maximum pit of 95 mils. Further investigation determined that the observed attack was largely due to a galvanic cell formed between the aluminum module and steel support framing. A zinc chromate coating had been specified to protect the aluminum panel in these areas but it afforded very little protection. The support framing on the new Mark 7 JBD's is aluminum which will eliminate the problem. On the older JBD's still in service, application of an effective, galvanically-compatible protective coating to the steel frame should eliminate the problem. Metallized aluminum or inorganic zinc with an epoxy topcoat are two coating systems that have demonstrated acceptable performance in tests simulating flight deck environments.



The top external side of the JBD module was in relatively good condition. When received, the module was heavily encrusted with a black carbonaceous residue. After removal of this residue, a few pits approaching 50 mils were detected. Other corrosion was minimal. There was evidence of mechanical impingement damage probably caused by foreign particles in the jet engine exhaust impacting on the panel face.

By far, the most significant corrosion occurred on the internal surfaces of the JBD panel. Figures 6 thru 9 show the typical attack. All wall penetrations were primarily caused by internal corrosion. On the bottom interior surface, numerous pits about 120 mils in depth were measured. An internal pit of 120 mils directly opposite an external pit of 40 mils would result in total penetration of the bottom wall (wall thickness is  $\approx$  150 mils). Many more penetrations would have occurred if the panel had remained in service. On an average, pit depths measured on the bottom interior surface were twice as great as pit depths measured on the top interior surface.

The wet chemical tests for copper gave positive results at each of the seven penetrations that had occurred on the bottom interior surface. However, no copper was evidenced in 6 separate tests conducted at randomly selected pits on the top interior surface. The interior surface of the JBD module also exhibited an obvious rust-colored surface film. The qualitative chemical test for iron gave positive results at every location tested.

Other areas of the Mark 6 JBD module showing severe corrosion were the inlet and outlet header pipes. The ends of the pipe had deteriorated to the point where the metal surface resembled a sponge (Figure 10). It appears that this attack is primarily due to crevice corrosion. Aluminum alloys are notoriously susceptible to crevice corrosion. A crevice is formed at the header pipe when non-metallic connecting hoses are clamped over the pipes. Use of a high temperature sealant at the connection joint might remedy the problem. There was no evidence of significant erosion attack on the internal surface of the header pipe at the 90° elbow. This would indicate the characteristic flow rates through the JBD panels are tolerable.

#### (2) MODULE RECEIVED FROM USS FORESTAL.

A module fabricated according to the Mark 7 design was returned to NAVAIRENGCEN from the USS Forrestal (CVA-59) after approximately 1 year of service. The panel was inspected for both external and internal corrosion.

When received, the panel was heavily encrusted with a black carbonaceous residue similar to the Mark 6-type module. After removal of this residue, general pitting of about 5 to 10 mils was obvious over the entire surface. Microscopic inspection indicated that some coating remained in a very few isolated areas but for the most part, the entire coating was gone. The panel had been flame-sprayed with a nickel-aluminide coating @ 10 mils. No evidence of galvanic corrosion was found on the underside of the panel as had been detected for the other panel. This panel was supported by aluminum framing rather than steel.

Again, the most significant corrosion occurred on the internal surfaces of the JBD module. Upon sectioning the module, corrosion products in the form of localized white blisters were evident on the interior surfaces. This is typical of aluminum corrosion. After wire brushing the panels, pitting was quite evident. The deepest pits that were measured approached 50 to 60 mils with average pitting about 30 mils. For the Mark 6 module, pitting was more frequent and deeper on the bottom interior surface. However, for this module, pitting occurred predominantly on one side of the panel centerline. The pitting on the bottom interior surface was slightly greater than on the top interior surface, however the difference was not nearly as noticeable as on the Mark 6 module. It could not be determined why pitting predominantly occurred on one side of the module centerline.

Again, qualitative chemical tests were made for copper and iron. In this case, all tests for copper proved negative. For iron, every test was again positive. The interior surfaces showed a similar rust-colored film as observed for the other module.

b. COOLING WATER ANALYSES. Table I summarizes the results of chemical tests conducted on JBD cooling water samples returned from different aircraft carriers. It is evident from Table I that significant concentrations of copper and iron are present in JBD cooling water. Normally, in sea water, the concentration of copper is about .003 ppm. The only sea water sample showing a normal copper concentration was the sea water taken from the intake line at the test site in Ocean City. All JBD water samples were abnormally high in copper concentration. This occurs because the cooling water is supplied from cupro-nickel fire water mains.

c. WELD SENSITIZATION TESTS. Table II presents electrochemical data gathered on weld test specimens exposed in sea water @ 200°F. The data shows there is

no potential difference between the base metal, heat-affected zone, or weld metal. Also, the local-action corrosion rates are not excessive. Based on this data, weld sensitization does not appear to be a problem.

The results of the accelerated exposure test also confirm this. After 6 hours immersion in the  $H_2O_2$ -NaCl solution, there was no evidence of localized corrosion on the weld section.

d. SCREENING TESTS ON CANDIDATE INTERNAL COATINGS

(1) SELECTION. The as-fabricated shape of the JBD modules constrains the choice of a protective coating for the internal surfaces. A coating that can be applied in a thin film by an immersion or flow-through process is required. It doesn't appear that anodizing could be accomplished in a conventional manner because of the geometry. Individual electrodes would probably have to be inserted through each flow channel. On a production basis, this may prove expensive. Fluidized bed or electrostatically-sprayed coatings do not seem applicable because of the tight tolerances and requirement for relatively thin-film coatings. The poor thermal conductivity of most of these coatings would be a major disadvantage.

Table III presents the candidate coatings selected for screening. The first nine coatings are chromate-type conversion coatings. Chromate conversion coatings are widely used on aluminum alloys to improve weathering resistance and also as a prime coat to improve topcoat adhesion. A chromate conversion coating could be applied to the JBD by an immersion or flow-through process and would be relatively inexpensive. The major question mark regarding the use of chromate conversion coatings was their stability at the temperatures encountered in the JBD. Chromate coatings are known to decrease in corrosion resistance as the temperature increases.

Two chemical treatments for modifying chromate coatings to increase high temperature stability were also examined. These treatments have been reported by Pearlstein<sup>2</sup>. One treatment includes a post dip in glycerin to partially insolubilize the chromate coating. The other treatment is a post dip in barium nitrate. It is hypothesized that reaction of the chromate film with the barium salt solution results in conversion of soluble chromate in the film to less soluble barium chromate which is less detrimentally affected by heat.

<sup>2</sup>Pearlstein, F. & M. R. D'Ambrosio, "Heat Resistant Chromate Conversion Coatings", a paper presented at the 3rd Mid-Atlantic Regional Technical Meeting, American Electroplaters Society, Tamiment, Pa., Sept. 1967.

Three epoxy-base coatings were selected for screening. The polyamide epoxy coatings have shown good durability in other NAVAIRENGCEN tests conducted in sea water environments. The epoxy-ester coatings were included at the suggestion of the manufacturer (Dupont). Each of the three coatings can be thinned down and applied at a low coating thickness by a flow-through process. Two of the coatings contain corrosion-inhibitive pigments (zinc chromate, zinc oxide).

Another coating system selected as a candidate was a water-base aluminum ceramic. This coating system is rated for service temperatures up to 1200°F. It is advantageous in that the aluminum pigment makes it more thermally conductive than the epoxy-base coatings.

The last coating system selected for the screening tests was anodized aluminum. The anodized coating was included as a benchmark. The application problems associated with anodizing have already been mentioned.

(2) TESTING. Table IV presents the data obtained from the screening tests. The data includes calculated corrosion rates on coated aluminum test coupons in sea water @ 100°C. The corrosion rates were determined by making polarization resistance measurements. The data shows that after 30 days in sea water @ 100°C, many of the coated test specimens exhibited a significantly lower corrosion rate than the uncoated control specimen. None of the coatings evidenced noticeable deterioration over 30 days. The chromate coated specimens did lose their gold iridescent color, becoming colorless within one day after immersion in sea water. This occurs when hexavalent chromium is reduced to its trivalent state.

The data as presented compares only general corrosion rates. It is useful in screening the performance of candidate coatings. However, aluminum usually pits rather than suffer general metal loss as evidenced by the JBD module inspection. In the 30-day screening tests, the uncoated control test specimen did not show pitting, indicating the test was not as severe as the JBD environment.

e. SIMULATED EXPOSURE TESTS. The simulated exposure tests were divided into 3 separate test runs. The first 2 test runs were 2 months in duration. The last test run was conducted for only 1 month.

Figure 11 presents a simplified schematic of the test loop conditions for the first test run. The flow

conditions represent the range of flows that are normally encountered in JBD operation. The test modules located downstream in each branch of the loop were coated. The coating system consisted of a chromate-conversion primer (Alodine<sup>(R)</sup>) and a polyamide-epoxy topcoat (Corlar<sup>(R)</sup>) @  $\approx$  1 mil dry film thickness. Four uncoated 6061-T6 aluminum pipe nipples were located in the test loop as shown in Figure 15. Electrochemical polarization measurements were made on each pipe nipple allowing determination of corrosion rates in situ.

Table V presents the corrosion rates determined initially. The effect of increasing the sea water temperature is obvious. The general corrosion rates increased between one and two orders of magnitude. Table V also indicates that sea water flowing @ 2.5 gpm is less corrosive than sea water flowing @ .5 gpm.

Table VI presents data obtained periodically over the course of the test run. The velocity effect is again evident. In general, corrosion rates were not abnormally high.

Upon completion of the first test run, the test modules were cut open and inspected for internal corrosion. There was no significant pitting of the interior surfaces (Figure 12). The conditions simulated during the first test run were not severe enough to cause the pitting rates observed on the JBD modules returned from the ships.

The epoxy coating applied to the two downstream modules blistered and disbonded. However, the temperature of the test modules had exceeded normal operating temperatures for a short period due to a malfunction in the test loop. This might have caused the coating failures. It was decided to retest the coating during the next test run.

The conditions for the second test run were identical except that copper was injected into the sea water. Saturated copper sulphate solution was injected at 5 ppm ahead of the test modules. Table VII presents corrosion rates calculated from the electrochemical data gathered during the second test run. The dramatic increase in corrosion rate compared to those determined during the first run is obvious. Inspection of the test modules on completion of the run confirmed the corrosion rates determined by polarization measurements. Extensive, deep pitting similar to that observed on actual modules was evident (Figure 13). Copper injected into the sea water appreciably

(R) Registered trademark of Amchem

(R) Registered trademark of E.I. Dupont & Co.

accelerated pitting. Based on the results of the second test run, it is believed that copper contamination in the JBD cooling water is the primary cause of internal corrosion. Chemical analyses of cooling water sampled from three different ships indicated that copper was present in all samples to varying degrees. Therefore, it is not unreasonable to anticipate accelerated internal pitting of the JBD's throughout the fleet.

Inspection of the coated test modules removed from the test loop showed the same degree of pitting corrosion (Figure 14). The epoxy coating @ 1 mil was obviously ineffective.

For the third test run, it was decided to evaluate the performance of other coatings that might be used to protect the internal surface from corrosion. The water-base aluminum ceramic coating was applied to the upstream modules in the test loop and a nitrile rubber coating was applied to the downstream modules. Both coatings were applied at  $\approx$  1 mil. Copper was again injected into the water.

Table VIII presents corrosion rates calculated from in situ electrochemical measurements. The data indicates that neither coating effected a significant decrease in corrosion rate. Inspection of the internal surfaces on completion of the test run again showed deep pitting and extensive coating deterioration. Based on the results of the test run, the use of either of these two coatings for controlling internal corrosion doesn't appear feasible.

f. HEAVY METAL FILTER TESTS. When it became apparent that the major cause of internal corrosion on the JBD's was copper contamination of the cooling water, tests were initiated to determine if an active metal filter could be used ahead of the JBD to remove copper from the cooling water. The use of ion-exchange resin to remove copper was ruled out because preliminary calculations indicated copious quantities of resin would be necessary. Assuming a flow of 1500 gpm through a Mark 7 JBD panel, 300 ft.<sup>3</sup> of resin would be required per panel in order to reduce the copper concentration by an order of magnitude. The calculations assumed a flow to resin ratio of 5 gpm/ft.<sup>3</sup> of resin. The resin considered for use was Amberlite<sup>(R)</sup> XE-318.

The beaker tests conducted to evaluate the use of active metal filters also indicated that impractical

<sup>(R)</sup> Registered trademark of Rohm & Haas Company

quantities of active metal (aluminum, zinc, or magnesium) would be required to reduce copper concentration to a low level. 190 gms of pure aluminum pellets added to 500 ml of copper-contaminated sea water did not effect a significant decrease in copper concentration after 30 minutes. Similar data were obtained for aluminum alloy (QQ-601-356) shavings, zinc pellets, and magnesium ribbon shavings.

To confirm the beaker tests, cartridge-type filters were made up of each active metal. The cartridge-type filters were made up with the maximum volume of metal to flow ratio that seemed practical for shipboard service. The filters were inserted in the test loop. Copper-contaminated sea water @ 3 gpm was pumped through each filter. None of the filters reduced the concentration of copper significantly.

It may be that other aluminum alloys might be more efficient as a filtering media for copper. Also, it would seem that an electrolytic-type filter could be made up to plate the copper out of solution. Further testing in this regard was beyond the scope of the present program.

### 3. CONCLUSIONS

a. Copper present in the sea water cooling supply significantly accelerates internal corrosion of the JBD's.

b. Copper originates in the sea water supply from copper-nickel (90-10) fire water mains located upstream of the JBD's.

c. With copper present in the sea water at the concentrations measured in this program (.1 to 10 ppm), the estimated service life of a Mark 7 JBD module is 2 to 4 years. If copper were not present in the sea water, the service life would exceed 20 years.

d. Chromate conversion coatings and organic, barrier-type coatings are ineffective in reducing the rate of internal corrosion on the JBD's. Other coatings not tested in this program (e.g. electroless nickel) might be effective in reducing copper-caused corrosion.

e. Removal of copper from the sea water by a filter (either ion exchange resin or active metal) appears to be impractical based on the rate of flow and amount of copper present. Other filtering techniques such as electroplating the copper out of solution might prove to be effective. Such testing was beyond the scope of this program.

#### 4. FUTURE ACTIONS

a. Future evaluations will be based on the results of efforts to determine the concentration of copper in the cooling water aboard operational carriers.

#### C. EVALUATION OF NON-SKID DECK COATINGS

##### 1. EXPERIMENTAL PROCEDURES

a. LITERATURE SEARCH. A literature search was conducted to determine metal-spray coatings that could be applied to the aluminum alloy JBD, exhibiting both non-skid and corrosion-resistant properties. Metal-spray coatings seem the most appropriate for the high temperature JBD environment based on prior work by NAVAIRENGCEN<sup>5</sup>.

On completion of the literature search, a meeting was held between representatives of NAVAIR, NAVSEA, and private industry in order to select candidate metal spray coatings for testing. Table IX presents the coatings selected for testing based on this meeting. The most important criteria for selection were: stability at intermittent temperatures approaching 1000 °C; non-skid characteristics; stability in a marine environment; and cost.

b. SIMULATED EXPOSURE TESTS. Exposure tests were conducted on the coatings selected from the literature search. The exposure tests were designed to determine the ability of the candidate coatings to withstand the typical carrier deck environment under realistically simulated conditions. Thirty (30) coatings were initially included in these tests. Nickel-aluminide, flame-sprayed at three different thicknesses, was introduced later in the tests. The duration of the tests was nine months.

The coatings were applied to 3" X 6" X 1/4" aluminum (6061-T6) test plates. All test plates were first sandblasted to ~1 mil profile. Prior to exposing the test plates, photographs were taken to characterize initial conditions. Electrochemical polarization and potential measurements were made initially and then repeated on a monthly basis as a means of detecting significant changes in coating performance (Appendix II). Figure 15 shows the set-up for making the measurements.

The test plates were exposed in an environment closely simulating that which the JBD is subjected to on the flight deck. The approximate time of the events in the daily exposure cycle was as follows:

<sup>5</sup> Moskowitz, "Development of Metallized Non-Skids For Jet Blast Detectors" NAEC Report No. 7849, August, 1974.



(1) 20 hours, 25 minutes: Marine atmosphere

(2) 1 hour: 1000°C hot jet blast, marine atmosphere cycle, with jet blast duration 5 seconds, marine atmosphere exposure 2 minutes, 55 seconds.

(3) 2 hours: Sea water immersion

(4) 5 minutes: Acidified sea water spray (8% sulphurous acid, by weight). This part of the exposure cycle simulates the effect of SO<sub>2</sub> stack gases reacting with sea water laying on the deck to form dilute sulphurous acid.

(5) 15 minutes: Simulated deck wash-down. Scrubbing with JP-5 jet fuel-detergent mixture, followed by sea water washing. Procedures were simulated as described in NAVSHIPS Technical Manual, Chapter 9140, 2 June, 1966, "Cleaning Method A".

(6) 15 minutes: Simulated deck exposure to contaminants. The test plates were wetted with lube oil, hydraulic fluid, and aircraft cleaning solution. The aircraft cleaning solution was a mixture of two cleaning compounds (MIL-C-43616 and MIL-C-25679) that are used on carrier aircraft.

To accomplish the above test cycle, a test rig as pictured in Figures 16 & 17 was built. The test plates were mounted horizontally on ceramic holders fastened to a 1/4-inch thick circular aluminum plate. Operation of the test rig was automatically controlled to effect the exposure cycle (excepting events (5) and (6) previously described). A timer circuit activated a fractional horsepower synchronous motor for 1 hour and 5 minutes a day. By coupling the aluminum plate to the motor through appropriate gears, the plate rotated at 1/3 rpm. During the 1 hour heat cycle, the test panels rotated under a jet nozzle burning liquid propane. In this manner, the panels received a hot jet blast ( $\approx$  1000°C) for 5 seconds duration. A blast of this duration caused a panel skin temperature of 200°C. For the acidified sea water spray event, the test panels rotated under a nozzle spraying acidified sea water. The spray was activated by using a separate timer circuit and solenoid valves. The two hour sea water immersion event was also accomplished using a timer circuit and solenoid valves. The remainder of the events in the exposure cycle were accomplished manually.

c. **ABRASION RESISTANCE TESTS.** Abrasion resistance tests were conducted according to the method described in ASTM D658-44. Figure 18 shows the general test set-up. The test consists of subjecting a coated test panel to an impinging stream of abrasive. The amount of abrasive required to wear the coating away to the bare metal is weighed and recorded. An abrasion coefficient is calculated for each coating as follows:

$$\text{Abrasion Coefficient} = \frac{\text{Abrasive Used, grams}}{\text{Coating Thickness, Mils}}$$

## 2. RESULTS

a. **SIMULATED EXPOSURE TESTS.** Table IX presents the coatings selected for evaluation in this phase of the program. Three types of metal spray process including flame-spray, electric arc-spray, and plasma-spray were used in applying the coatings. Duplicate test panels of each coating were prepared by Metco, Inc.

Some coatings were given a high profile texture to improve non-skid characteristics. Other coatings were sprayed to effect a diamond plate-type surface. The diamond plate pattern was produced by laying a wire mesh screen over the test panel and then applying the coating.

As is evident in Table IX, it was intended that some of the candidate coatings be tested at several thicknesses or with different surface profiles. On receiving the coated test panels from Metco, the total thickness of each coating system was determined by micrometer measurements. The data indicates that some of the coatings were applied much heavier than had been intended. Where more than one coating had been applied as part of a total system, it was impossible to measure the thickness of the individual coatings.

Table X summarizes the results of the simulated exposure tests. The coatings exhibiting the best performance include arc-sprayed aluminum, arc-sprayed aluminum-molybdenum, and arc-sprayed aluminum-titanium. Arc-sprayed aluminum was tested at different thicknesses; textured and patterned; over a flash coat of nickel-aluminide; over a bonding coat of molybdenum; and with a sealer coat. The aluminum-molybdenum coating was tested at 2 different compositions (50% Al-50% Mo. & 80% Al-20% Mo.) and also with a high profile texture. There was no observable deterioration of these coatings.

The nickel-aluminide coatings when applied at less than about 15 mils showed good resistance to the test environment. Aluminum corrosion products in the form of white blisters appeared on the surface over the test period (Figure 19). Additional deterioration was not detectable. Galvanic cell action between aluminum and nickel accelerates corrosion of the aluminum in the subject environment. Aluminum by itself did not show nearly as much corrosion product.

At thicknesses above 15 mils, the nickel-aluminide coating disbonded and delaminated (Figures 20 & 21). It appears that nickel-aluminide should not be applied at coating thicknesses exceeding 15 mils.

The arc-spray aluminum-nickel coating also showed white aluminum corrosion products but other than that was acceptable. The wire-spray aluminum coating (Metco No. 120) exhibited blistering after about 1 month in test (Figure 22). As documented in Table X, all other coatings included in the test performed poorly.

b. INTERPRETATION OF ELECTROCHEMICAL MEASUREMENTS. The electrochemical measurements included in the program as one means of quantifying coating performance correlated well with visual observations. Table XI presents corrosion rates determined in sea water at different intervals during the exposure test. Table XII presents electrochemical potentials.

In general, the initial corrosion rate determined for aluminum-coated panels was lower by an order of magnitude than most of the other coatings. The high profile arc-sprayed aluminum coating corroded initially at  $\approx 6$  mpy, however after the first month in test, the corrosion rate had dropped to  $\approx .7$  mpy. On the average, the corrosion rate for the aluminum coatings approached a steady-state rate of about .5 mpy. The aluminum-molybdenum coatings also approached a steady-state rate of around .5 mpy. The high profile aluminum-molybdenum coating corroded initially at  $\approx 2$  mpy, but decreased with time to  $\approx .5$  mpy. The aluminum-titanium coating averaged about .1 mpy over the test period.

The coatings exhibiting poor performance based on visual inspection generally corroded at significantly greater rates. For example, the aluminum-zinc coatings corroded at  $\approx 2$  to 4 mpy throughout the test. As a reference, the corrosion rate of uncoated steel in sea water is approximately 5 mpy.

The measured corrosion rate for the alumina-titania coating was low throughout the test. However, the

coating failed, disbonding over  $\approx 50\%$  of the panel (Figure 23). The alumina-titania coated panel exhibited a low corrosion rate because alumina and titania are both cermet. Thus, the coating acted more as a barrier-type coating than a metallic-type coating. The measurements actually reflect the corrosion rate of the 6061-T6 aluminum substrate at pinholes or "holidays" in the barrier-type coating. As the coating disbonded, the exposed substrate area was increased and the corrosion rate increased toward a rate more characteristic of the 6061-T6 alloy in sea water.

The electrochemical data clearly demonstrates the effect of the silicone sealer. In every case, where a comparison is possible, the silicone sealer initially lowers the corrosion rate. However, after one month, the beneficial effects of the sealer coat are no longer apparent. This was not obvious by visual inspection. Based on this data, use of the sealer coat does not seem cost effective.

The electrochemical potential data is also helpful in assessing coating performance. For example, the initial potential of the aluminum-zinc coatings was  $\approx -1.00$  to  $-1.10$  volts. Potentials in this range are characteristic of zinc in sea water. The zinc phase of the coating is more active and less resistant to corrosion in sea water. As the exposure test progressed, the potentials of the aluminum-zinc coatings shifted toward more noble values indicating that the zinc was being sacrificially depleted from the coatings. Visually, the coatings showed excessive corrosion over 9 months.

c. ABRASION RESISTANCE TESTS. Figure 24 is a bar chart summarizing the results of the abrasion resistance tests. From averaging the data, the nickel-aluminide coatings appear to be the most resistant to abrasion.

### 3. CONCLUSIONS

a. Based on the simulated exposure tests, arc-sprayed aluminum, arc-sprayed aluminum molybdenum, and arc-sprayed aluminum titanium are the most resistant to the flight deck environment. Arc-sprayed aluminum appears optimum from a cost standpoint.

b. Flame-sprayed nickel aluminide exhibits the best abrasion resistance. It is not as resistant to the flight deck environment as the coatings identified in a. above.

c. Determination of the optimum non-skid coating depends on the results of in-service performance tests now in progress on different aircraft carriers.

#### 4. FUTURE ACTIONS

a. Future development efforts will be based on Fleet test results.

TABLE I - JBD COOLING WATER ANALYSIS FOR  
IRON AND COPPER

	<u>Ship/Sampling Point</u>	<u>Iron, ppm</u>	<u>Copper, ppm</u>
1.	CVA 63/Cat. No. 1, JBD outlet	.01	.08
2.	CVA 63/Cat. No. 1, JBD inlet	.02	1.24
3.	CVA 63/Cat. No. 3, JBD inlet	.01	1.24
4.	CVA 63/Cat. No. 3, JBD outlet	.76	8.0
5.	CVA 64/Cat. No. 3, JBD outlet	.01	.05
6.	CVA 64/Cat. No. 3, JBD inlet	.24	1.68
7.	CVA 64/Cat. No. 4, JBD outlet	.02	.08
8.	CVS 14/JBD inlet	3.52	.98
9.	CVS 14/JBD outlet	12.6	6.0
10.	Intake water @ Ocean City	.03	<.01

TABLE II - LOCAL ACTION CORROSION RATES AND  
POTENTIALS FOR WELD TEST SPECIMENS

	<u>Corrosion Rate,</u> <u>mpy</u>	<u>Potential,</u> <u>Volts, SCE</u>
Base Metal	.441	-.56v
Heat Affected Zone	.738	-.56v
Weld Metal	.974	-.56v

TABLE III - CANDIDATE COATINGS FOR USE ON THE INTERNAL SURFACES OF THE JBD

<u>Coating</u>	<u>Supplier</u>	<u>Mil-Spec</u>
1. Alodine 1200	Amchem	MIL-C-81706
2. Bonderite 723	Parker Company	"
3. Divercoat	Diversery Corp.	"
4. Corcoat	Coral Chemical Company	"
5. Chromicoat L25	Oakite Products, Inc.	"
6. Albond Q	Pennwalt Corp.	N/A
7. Hinac BK 1-F	Pennwalt Corp.	N/A
8. Alodine 1200 + Glycerine	Amchem	MIL-C-81706 N/A
9. Alodine 1200 + Barium Nitrate	Amchem	MIL-C-81706 N/A
10. Polyamide-Epoxy (Zinc Chromate Pigment)	Dupont	N/A
11. Epoxy Ester (Zinc Oxide Pigment)	Dupont	N/A
12. Epoxy Ester	Dupont	N/A
13. Aluminum-Ceramic (Water Base)	CFI, Inc.	N/A
14. Anodized Aluminum	N/A	N/A



TABLE IV - GENERAL CORROSION RATES\* FOR COATED  
6061-T6 ALUMINUM TEST COUPONS IN SEA  
WATER @ 100°C

<u>Coating</u>	<u>Corrosion Rate, mpy</u>	
	<u>Initial</u>	<u>30 days</u>
1. No coating (control)	.843	.0957
2. Alodine 1200S	.139	.0038
3. Bonderite 723	.011	.0042
4. Divercoat	.018	.0058
5. Corcoat	.026	.032
6. Albond Q	.018	.0058
7. Hinac	.820	.023
8. Anodized Aluminum	.0048	.0016
9. Chromicoat LC-25	.043	.0034
10. Alodine + Glycerine	.044	.0173
11. Alodine + Barium Nitrate	.174	.407
12. Epoxy-Ester	.0072	.0067
13. Polyamide Epoxy	.0448	.0020
14. Epoxy Ester (ZnO)	.0022	.0014
15. Aluminum Ceramic	.0054	.0033

\*Determined by polarization resistance measurements.

TABLE V - INITIAL CORROSION RATE DATA FOR JBD TEST LOOP\*

	<u>Pipe Nipple A</u>	<u>Pipe Nipple B</u>	<u>Pipe Nipple C</u>	<u>Pipe Nipple D</u>
Sea Water (no flow @ 25°C)	.045 4mpy	.0502 mpy	.0128 mpy	.0208 mpy
Sea Water (flowing @ 10°C)	.0367 mpy	.0125 mpy	.0273 mpy	.0273 mpy
Sea Water (flowing @ 100°C)	1.36 mpy	4.30 mpy	.244 mpy	.654 mpy

\*See Figure 11 for schematic of JBD Test Loop

TABLE VI - PERIODIC CORROSION RATE DATA FOR JSD TEST LOOP (RUN NO. 1)

	<u>Pipe Nipple A</u>	<u>Pipe Nipple B</u>	<u>Pipe Nipple C</u>	<u>Pipe Nipple D</u>
<u>Initial</u>	1.36 mpy	4.30 mpy	.244 mpy	.654 mpy
4 weeks in test	.41"	2.04"	.193"	.185"
5 weeks in test	.56"	.88"	.216"	.289"
6 weeks in test	.44"	1.10"	.216"	.289"
7 weeks in test	.24"	2.19"	.156"	.224"
8 weeks in test	.52"	2.41"	.213"	.181"
9 weeks in test	.51"	4.40"	.769"	.454"

TABLE VII - PERIODIC CORROSION RATE DATA FOR JBD TEST 1000 (RUN NO. 2)

	<u>Pipe Nipple A</u>	<u>Pipe Nipple B</u>	<u>Pipe Nipple C</u>	<u>Pipe Nipple D</u>
<u>Initial</u>	1.18 mpy	2.26 mpy	1.34 mpy	.842 mpy
1 week in test	2.09"	.218"	.656"	.347"
2 weeks in test	1.99"	.222"	1.82"	.128"
3 weeks in test	13.74"	65.44"	22.64"	64.93"
4 weeks in test	9.16"	59.61"	24.28"	44.91"

TABLE VIII - PERIODIC CORROSION RATE DATA FOR JBD TEST LOOP (RUN NO. 3)

	Pipe <u>Nipple A</u>	Pipe <u>Nipple B</u>	Pipe <u>Nipple C</u>	Pipe <u>Nipple D</u>
<u>Initial</u>	4.16 mpy	49.1 mpy	10.9 mpy	16.95 mpy
1 week in test	14.11"	29.6"	11.24"	21.8"
2 weeks in test	15.79"	21.53"	7.76"	26.01"
3 weeks in test	6.15"	16.84"	8.37"	20.72"
4 weeks in test	8.90"	18.96"	2.20"	13.35"

TABLE IX - CANDIDATE NON-SKID COATINGS SELECTED FOR TESTING

<u>Coating And Recommended Thickness</u>		<u>Measured Total Thickness (Mils)</u>
1.	Flame-Sprayed Nickel-Aluminide @ 5 mils	9.5
2.	Flame-Sprayed Nickel-Aluminide @ 15 mils	19.5
3.	Flame-Sprayed Nickel-Aluminide @ 4-6 mils Flame-Sprayed Zinc @ 2-5 mils Flame-Sprayed Nickel-Aluminide @ 4-6 mils	15.5
4.	Flame-Sprayed Nickel-Aluminide @ 4-6 mils Flame-Sprayed Zinc @ 2-5 mils Flame-Sprayed Nickel-Aluminide @ 10 mils	15.5
5.	Flame-Sprayed Nickel-Aluminide @ 4-6 mils Flame-Sprayed Aluminum @ 5 mils Flame-Sprayed Nickel-Aluminide @ 5 mils	25.5
6.	Flame-Sprayed Nickel-Aluminide @ 10 mils Flame-Sprayed Aluminum @ 2 mils	31.5
7.	Arc-Sprayed Aluminum - Textured @ 30 mils	16.0
8.	Arc-Sprayed Aluminum - Textured @ 30 mils w/Silicone Sealer	34.0
9.	Arc-Sprayed Aluminum Nickel (50% Al - 50% Ni) - Textured @ 15 mils	8.5
10.	Arc-Sprayed Aluminum Molybdenum (50% Al - 50% Moly) - Textured @ 15 mils	20.5

TABLE IX (Cont'd.)

<u>Coating And Recommended Thickness</u>		<u>Measured Total Thickness (Mils)</u>
11.	Arc-Sprayed Aluminum Molybdenum (80% Al - 20% Moly) - Textured @ 15 mils	28.0
12.	Arc-Sprayed Aluminum Nichrome (50% Al - 50% Nichrome) - Textured @ 15 mils	24.5
13.	Arc-Sprayed Aluminum Zinc (50% Al - 50% Zn) - Textured @ 15 mils	15.0
14.	Arc-Sprayed Aluminum Zinc (80% Al - 20% Zn) - Textured @ 15 mils	19.0
15.	Flame-Sprayed Nickel-Aluminide @ 4-6 mils Arc-Sprayed Aluminum - Textured @ 15 mils	30.0
16.	Flame-Sprayed Nickel-Aluminide @ 4-6 mils Arc-Sprayed Molybdenum - Textured to 15 mils	19.5
17.	Arc-Sprayed Molybdenum @ 4-6 mils Arc-Sprayed Aluminum - Textured @ 15 mils	21.0
18.	Arc-Sprayed Aluminum - Textured @ 15 mils w/Silicone Sealer	61.0
19.	Flame-Sprayed Nickel-Aluminide (Flash Coat) Arc-Sprayed Aluminum - Textured @ 15 mils w/Silicone Sealer	55.0
20.	Flame-Sprayed Nickel-Aluminide - Patterned @ 15 mils w/Silicone Sealer	11.6

TABLE IX (Cont'd.)

<u>Coating And Recommended Thickness</u>		<u>Measured Total Thickness (Mils)</u>
21.	Plasma-Sprayed Alumina Titania (50% $Al_2O_3$ - 50% $TiO_2$ ) @ 5-8 mils	7.5
22.	Plasma-Sprayed Aluminum Titanium (50% Al - 50% Ti) @ 5-8 mils	7.0
23.	Flame-Sprayed Aluminum @ 15 mils	15.5
24.	Flame-Sprayed Multiphase Alloy @ 15 mils w/Silicone Sealer	7.5
25.	Arc-Sprayed Aluminum Molybdenum (50% Al - 50% Moly) @ 15 mils	33.0
26.	Plasma-Sprayed Nickel Titanium (50% Ni - 50% Ti) @ 15 mils	7.5
27.	Arc-Sprayed Aluminum Zinc (50% Al - 50% Zn) - Textured @ 30 mils w/Silicone Sealer	43.0
28.	Flame-Sprayed Nickel Aluminide (Flash Coat) Flame-Sprayed Aluminum - Patterned @ 15 mils w/Silicone Sealer	5.1
29.	Flame-Sprayed Nickel-Aluminide - Textured @ 12 mils w/Silicone Sealer	24.0
30.	Arc-Sprayed Aluminum Nickel (50% Al - 50% Ni) - Textured @ 15 mils w/Silicone Sealer	7.0



TABLE IX (Cont'd.)

<u>Coatings And Recommended Thickness</u>		<u>Measured Total Thickness (Mils)</u>
31.	Flame-Sprayed Nickel-Aluminide	7.0
32.	Flame-Sprayed Nickel-Aluminide	10.0
33.	Flame-Sprayed Nickel Aluminide	14.0

TABLE A - GENERAL DESCRIPTION OF METAL-SPRAY COATING PERFORMANCE

No.	Description	Remarks
1.	Ni-Al	Good (light blistering 2 weeks into test)
2.	Ni-Al	Failed (severe blistering 2 days into test, removed from test after 4 weeks)
3.	Ni-Al:Zn:Ni-Al	Failed (severe blistering 2 weeks into test, removed from test after 4 weeks)
4.	Ni-Al:Zn:Ni-Al	Failed (severe blistering 2 weeks into test, removed from test after 3 weeks)
5.	Ni-Al:Al:Ni-Al	Poor (blistering, checking and cracking 2 weeks into test)
6.	Ni-Al:Al	Poor (blistering, peeling and cracking 4 weeks into test)
7.	Al	Very good
8.	Al:SA	Very good
9.	Al-Ni (50-50)	Good (corrosion products and pinholes 10 weeks into test)
10.	Al-Moly (50-50)	Good (corrosion products 17 weeks into test)
11.	Al-Moly (80-20)	Very good
12.	Al-NiCr (50-50)	Failed (blistering 2 weeks into test, removed from test after 4 weeks)

TABLE X (Cont'd.)

No.	<u>Description</u>	<u>Remarks</u>
13.	Al-Zn (50-50)	Failed (blistering 7 weeks into test, peeling 8 weeks into test, removed from test after 17 weeks with 95% of coating delaminated)
14.	Al-Zn (80-20)	Failed (heavy corrosion products after 3 weeks into test)
15.	Ni-Al:Al	Very good
16.	Ni-Al:Moly	Failed (blistering 2 weeks into test, peeling after 8 weeks)
17.	Moly:Al	Good (corrosion products 17 weeks into test with light blistering and checking)
18.	Al:SA	Very good
19.	Ni-Al:Al:SA	Very good
20.	Ni-Al:SA	Failed (cracking, peeling, flaking, some delamination after 9 weeks in test)
21.	$\text{Al}_2\text{O}_3\text{-TiO}_2$ (50-50)	Failed (flaking on edges after 9 weeks, 90% peeling 12 weeks into test, blistering after 9 weeks)
22.	Al-Ti (50-50)	Very good
23.	Al	Fair (light blistering 3 weeks into test)

TABLE X (Cont'd.)

No.	<u>Description</u>	<u>Remarks</u>
24.	MP:SA	Poor slight cracking 2 weeks into test with medium blistering and checking)
25.	Al-Moly (50-50)	Very good
26.	Ni-Ti (50-50)	Poor (blistering, checking, and cracking 2 weeks into test)
27.	Al-Zn:SA	Failed (heavy corrosion products 2 weeks into test, blistering after 7 weeks, peeling and flaking 9 weeks into test)
28.	Ni-Al:Al:SA	Very good
29.	Ni-Al:SA	Failed (blistering, cracking and disbonding 3 weeks into test)
30.	Al-Ni (50-50):SA	Fair (medium blistering 3 weeks into test)
31.	Ni-Al	Good
32.	Ni-Al	Good
33.	Ni-Al	Good

TABLE XI - PERIODIC CORROSION RATES (MPY) FOR METAL SPRAY EXPOSURE PANELS

No.	Description	Initial	1 MO	2 MO	3 MO	4 MO	5 MO	9 MO
1.	Ni-Al	3.22	1.20	.605	.508	.807	.915	*
2.	Ni-Al	3.94	2.74	*	*	*	*	*
3.	Al-Zn-Al	3.22	1.83	*	*	*	*	*
4.	Al-Zn-Al	3.95	*	*	*	*	*	*
5.	Ni-Al:Al:Ni-Al	4.12	3.02	.699	.616	1.49	1.76	*
6.	Ni-Al:Al	3.13	1.51	1.36	.657	1.70	1.44	*
7.	Al	.864	.181	.158	.038	.158	.103	.084
8.	Al:SA	.048	.241	.131	.029	.181	.169	.155
9.	Al-Ni (50-50)	1.04	.910	.526	.088	.504	.453	*
10.	Al-Moly (50-50)	.562	.604	.403	.126	.406	.368	.317
11.	Al-Moly (80-20)	.180	.212	.151	.061	.833	.269	.212
12.	Al-NiCr (50-50)	.298	6.65	*	*	*	*	*
13.	Al-Zn (80-20)	3.41	2.62	.026	2.07	2.37	*	*
14.	Al-Zn (80-20)	2.57	3.02	3.85	3.23	3.11	3.02	*
15.	Ni-Al:Al	5.73	.670	1.65	.050	.269	.050	.185

TABLE XI (Cont'd.)

No.	Description	Initial	1 MO	2 MO	3 MO	4 MO	5 MO	9 MO
16.	Ni-Al:Moly	2.84	1.51	1.30	.448	.839	1.51	*
17.	Moly-Al	.726	.544	.570	.151	.519	.631	.325
18.	Al:SA	.070	.102	.259	.035	.223	.355	.143
19.	Ni-Al:Al:SA	.409	.241	.330	.227	.909	.670	.234
20.	Ni-Al:SA	1.41	2.01	.992	.468	1.58	2.52	*
21.	Al <sub>2</sub> O <sub>3</sub> -TiO <sub>2</sub> (50-50)	.0099	.027	.023	.012	.110	*	*
22.	Al-Ti (50-50)	.124	.270	.091	.023	.081	.132	.064
23.	Al	.153	.302	.151	.020	.063	.168	.130
24.	MP:SA	.270	.604	.519	.154	.259	.756	*
25.	Al-Moly (50-50)	2.08	1.20	.647	.147	.861	.605	.402
26.	Ni-Ti (50-50)	6.31	1.09	.667	.234	.463	.726	*
27.	Al-Zn:SA	3.16	10.4	7.93	.533	1.56	*	*
28.	Ni-Al:Al:SA	.104	.702	.279	.172	.839	.844	.448
29.	Ni-Al:SA	.845	3.02	2.12	4.91	5.16	5.73	*
30.	Al-Ni (50-50):SA	.347	.302	.340	.108	.313	.355	*

TABLE XI (Cont'd.)

<u>No.</u>	<u>Description</u>	<u>Initial</u>	<u>1 MO</u>	<u>2 MO</u>	<u>3 MO</u>	<u>4 MO</u>	<u>5 MO</u>	<u>9 MO</u>
31.	Ni-Al**	.089	.855	1.04				
32.	Ni-Al**	.166	.388	.474				
33.	Ni-Al**	.145	.414	1.22				

\*Testing discontinued

\*\*Placed in test 3 months after start of exposure tests

TABLE XII - PERIODIC CORROSION POTENTIALS<sup>†</sup> FOR METAL SPRAY EXPOSURE PANELS

No.	Description	Initial	1 MO	2 MO	3 MO	4 MO	5 MO	9 MO
1.	Ni-Al	.715	.690	.750	.755	.745	.722	*
2.	Ni-Al	.715	.690	*	*	*	*	*
3.	Al:Zn:Al	.865	.800	*	*	*	*	*
4.	Al:Zn:Al	.785	*	*	*	*	*	*
5.	Ni-Al:Al:Ni-Al	.795	.735	.760	.765	.750	.748	*
6.	Ni-Al:Al	.965	.695	.762	.801	.750	.761	*
7.	Al	1.01	.662	.771	.812	.772	.790	.775
8.	Al:SA	.790	.670	.771	.821	.720	.807	.790
9.	Al-Ni (50-50)	.720	.682	.752	.762	.700	.742	*
10.	Al-Moly (50-50)	.860	.651	.770	.782	.713	.758	.755
11.	Al-Moly (80-20)	.833	.659	.773	.769	.680	.740	.760
12.	Al-NiCr (50-50)	.620	.695	*	*	*	*	*
13.	Al-Zn (50-50)	1.10	.791	.869	.829	.782	*	*
14.	Al-Zn (80-20)	1.08	.920	.940	.866	.870	.832	*
15.	Ni-Al:Al	.958	.780	.829	.810	.778	.751	.760



TABLE XII (Cont'd.)

No.	Description	Initial	1 MO	2 MO	3 MO	4 MO	5 MO	9 MO
16.	Ni-Al:Moly	.698	.700	.799	.791	.760	.759	*
17.	Moly-Al	.962	.750	.778	.788	.740	.779	.759
18.	Al:SA	.740	.675	.772	.815	.716	.760	.795
19.	Ni-Al:Al:SA	.812	.720	.765	.814	.798	.788	.780
20.	Ni-Al:SA	.710	.780	.772	.758	.748	.752	*
21.	Al <sub>2</sub> O <sub>3</sub> -TiO <sub>2</sub> (50-50)	.700	.731	.790	.815	.711	*	*
22.	Al-Ti (50-50)	.725	.760	.790	.819	.763	.789	.752
23.	Al	.798	.700	.749	.818	.744	.722	.760
24.	MP:SA	.615	.700	.755	.760	.695	.638	*
25.	Al-Moly (50-50)	.705	.725	.776	.800	.700	.748	.750
26.	Ni-Ti (50-50)	.715	.785	.775	.775	.700	.738	*
27.	Al-Zn:SA	1.06	.980	1.03	.745	.758	*	*
28.	Ni-Al:Al:SA	.851	.830	.758	.791	.740	.768	.735
29.	Ni-Al:SA	.715	.815	.755	.887	.816	*	*
30.	Al-Ni (50-50):SA	.702	.760	.751	.749	.713	.741	*

TABLE XII (Cont'd.)

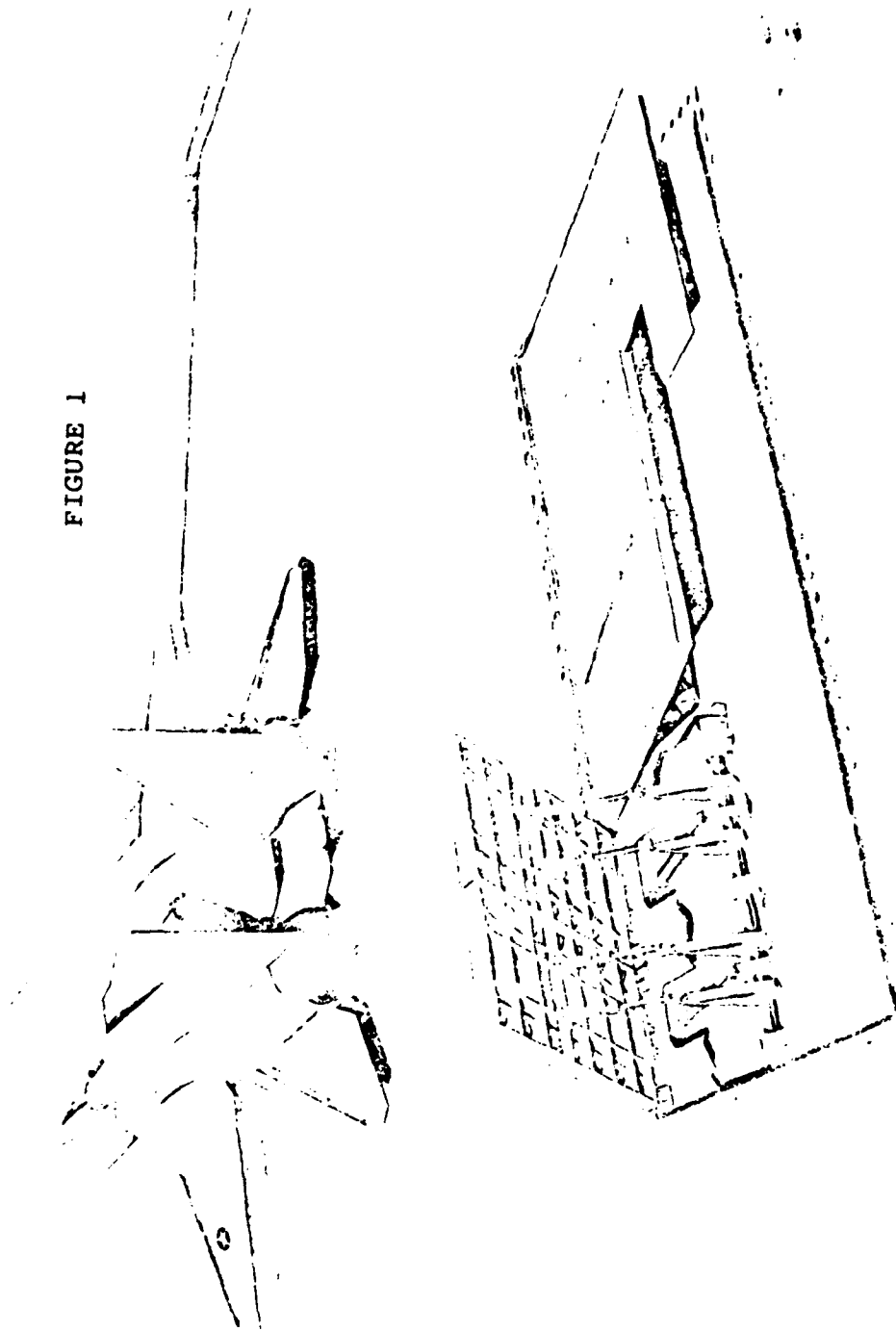
<u>No.</u>	<u>Description</u>	<u>Initial</u>	<u>1 MO</u>	<u>2 MO</u>	<u>3 MO</u>	<u>4 MO</u>	<u>5 MO</u>	<u>9 MO</u>
31.	Ni-Al**	.700	.741	.695				
32.	Ni-Al**	.735	.675	.675				
33.	Ni-Al**	.650	.721	.842				

+All potentials expressed in negative absolute volts with respect to Ag-AgCl reference cell

\*Testing discontinued

\*\*Placed in test 3 months after start of exposure tests

FIGURE 1



F-14 AT MK 7 JET BLAST DEFLECTOR NO.1

DESIGNED BY ARMY AIR ENGINEERING CENTER  
PHILADELPHIA, PA.

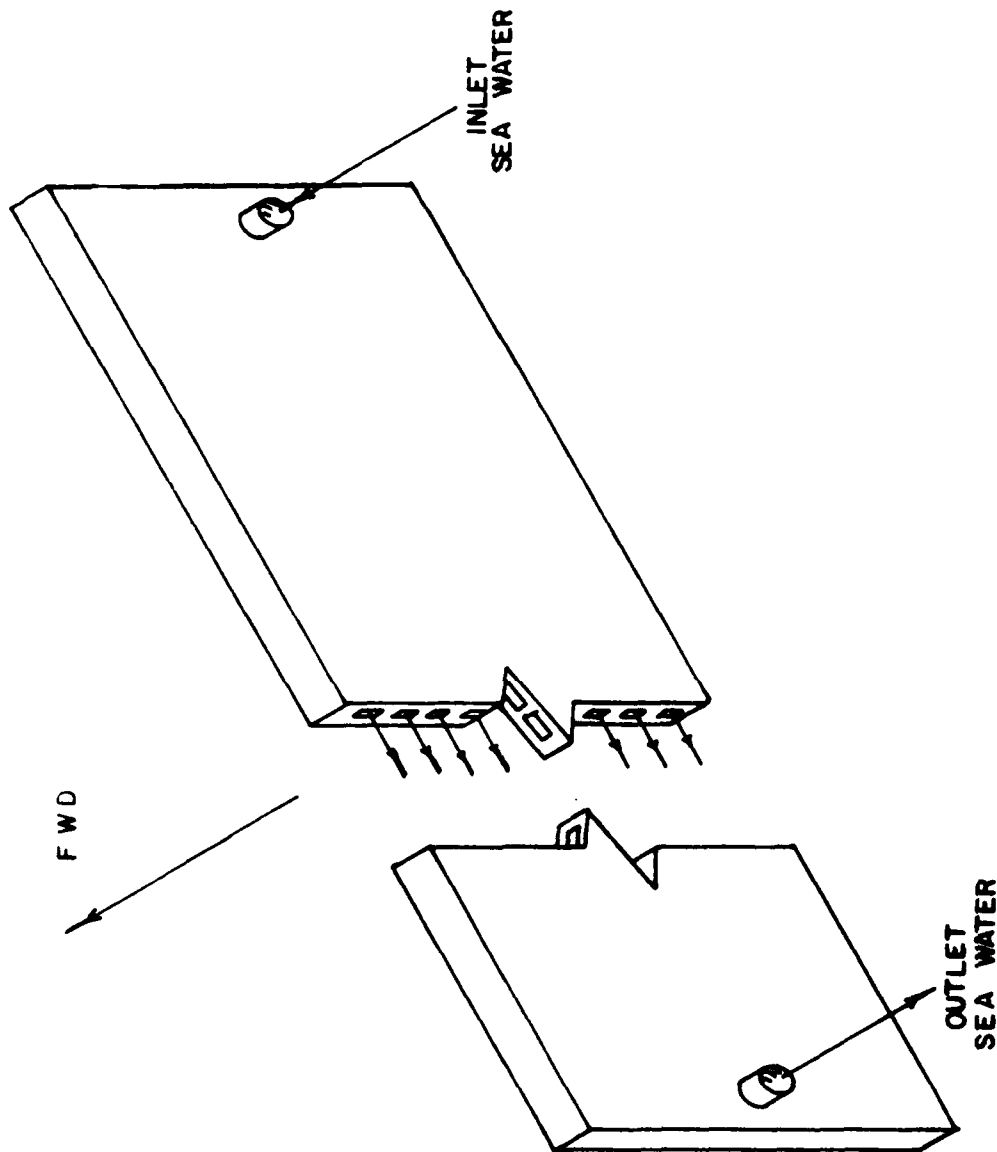


FIGURE 2 - 2' X 6' ALUMINUM MODULE SECTION  
USED TO ASSEMBLE JBD.

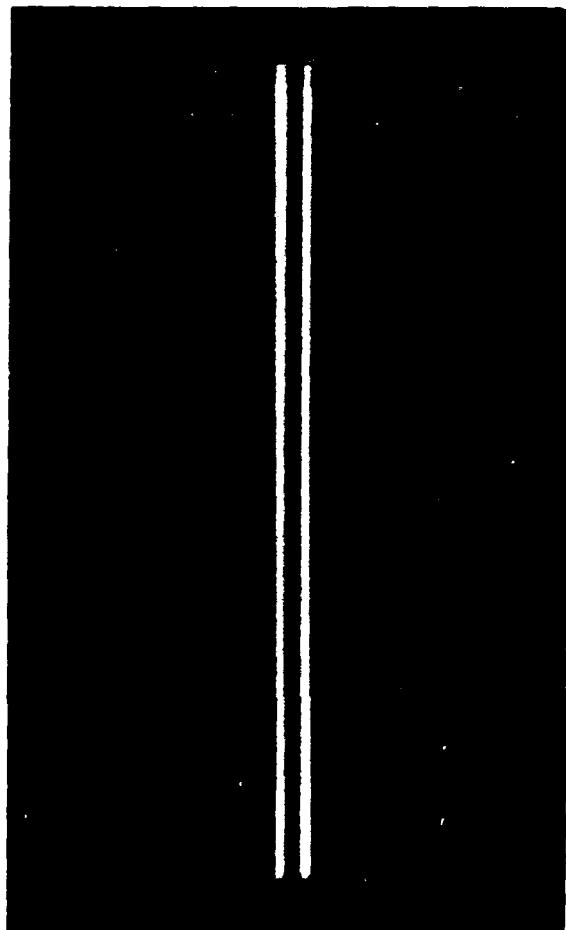


FIGURE 3 - Test Specimen Used in Screening  
Tests for Internal Coatings

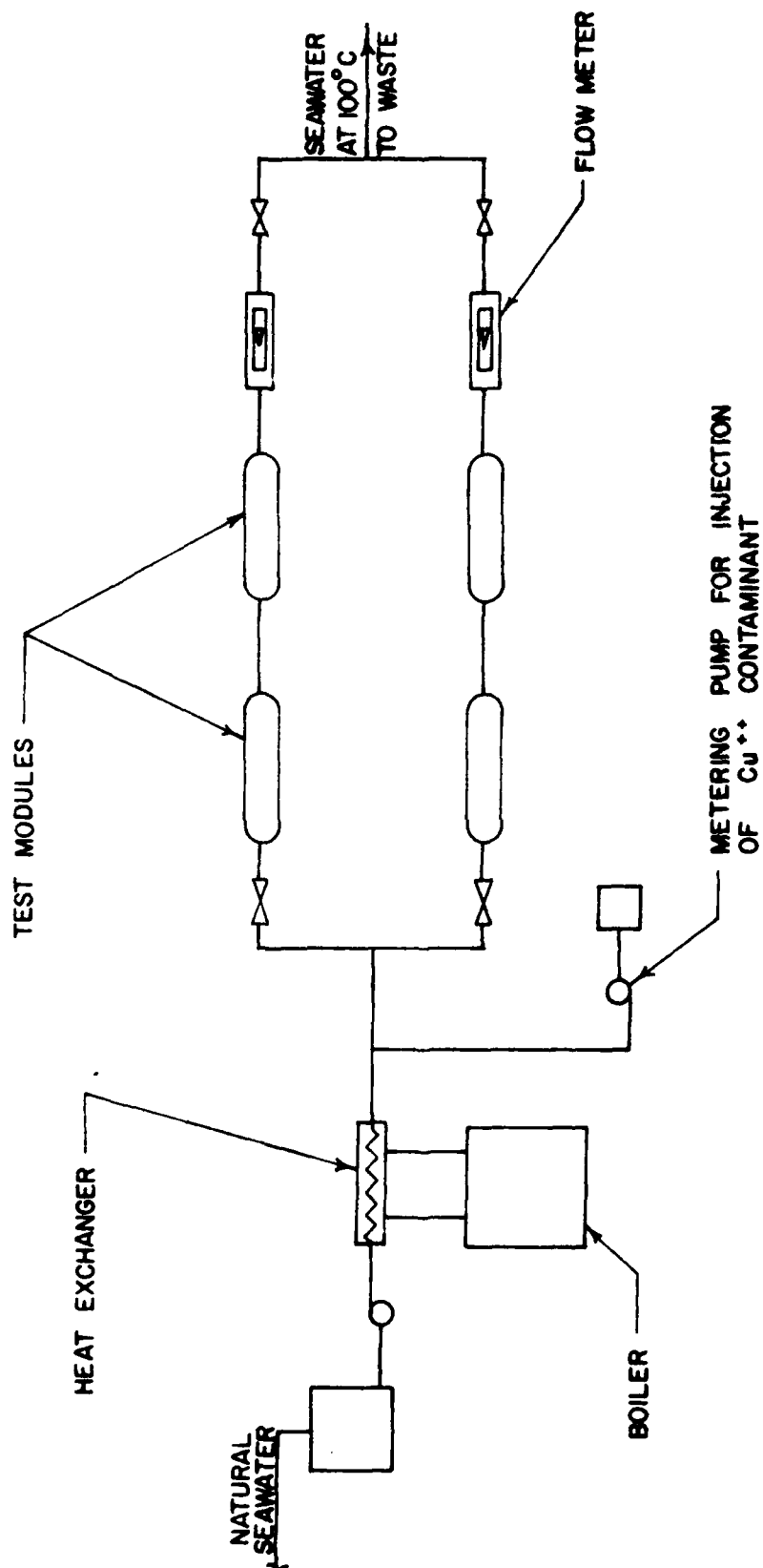


FIGURE 4 - TEST LOOP FOR SIMULATING INTERNAL CORROSION OF THE JBD'S

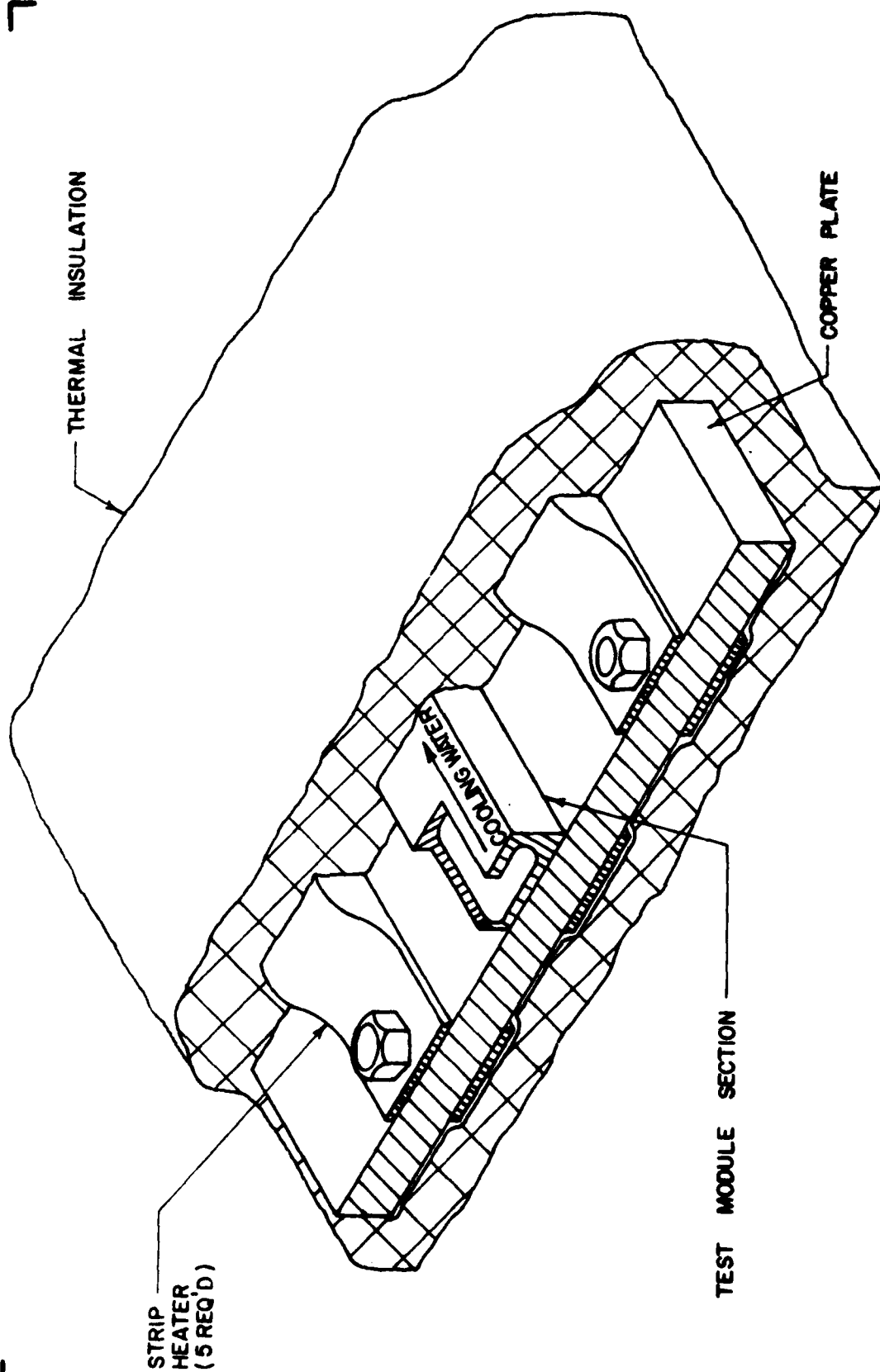


FIGURE 5 - ARRANGEMENT FOR HEATING TEST MODULE SECTION



FIGURE 7 - Internal Corrosion Attack  
on Mark 6 JBD Panel Removed  
From USS Kitty Hawk



FIGURE 6 - Internal Corrosion Attack  
on Mark 6 JBD Panel Removed  
From USS Kitty Hawk





FIGURE 9 - Internal Corrosion Attack  
on Mark 6 JBD Panel Removed  
From USS Kitty Hawk

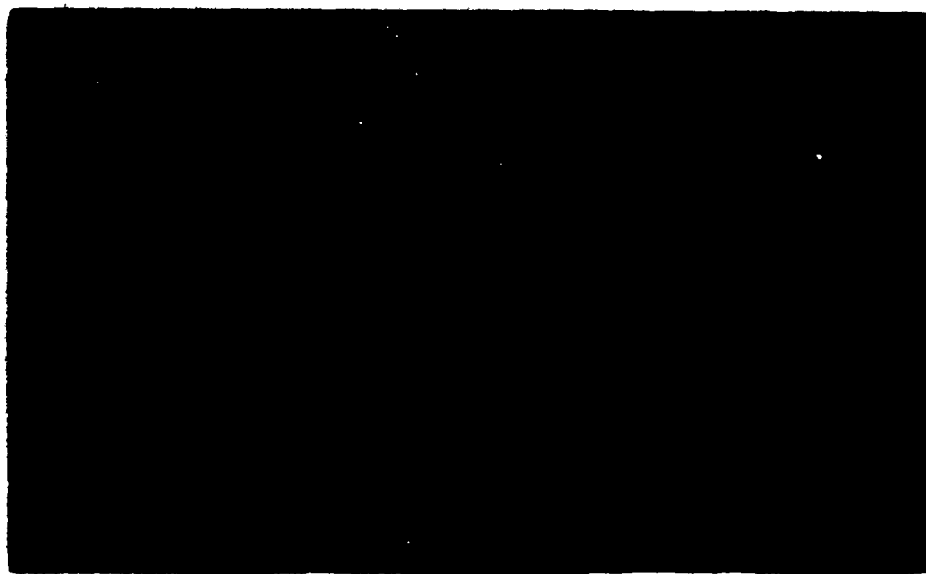


FIGURE 8 - Internal Corrosion Attack  
on Mark 6 JBD Panel Removed  
From USS Kitty Hawk



FIGURE 10 - Corrosion Attack on Inlet Pipe on  
Mark 6 JBD Panel Removed From  
USS Kitty Hawk

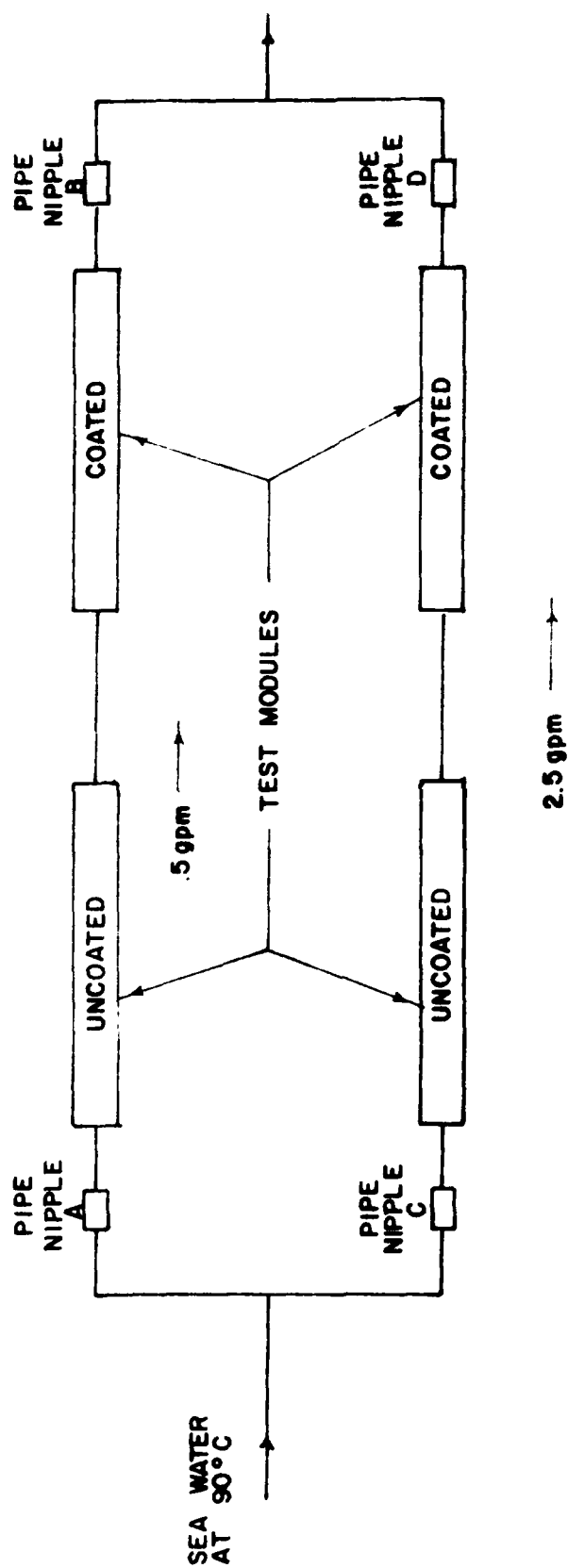


FIGURE II-SIMPLIFIED SCHEMATIC OF JBD TEST LOOP

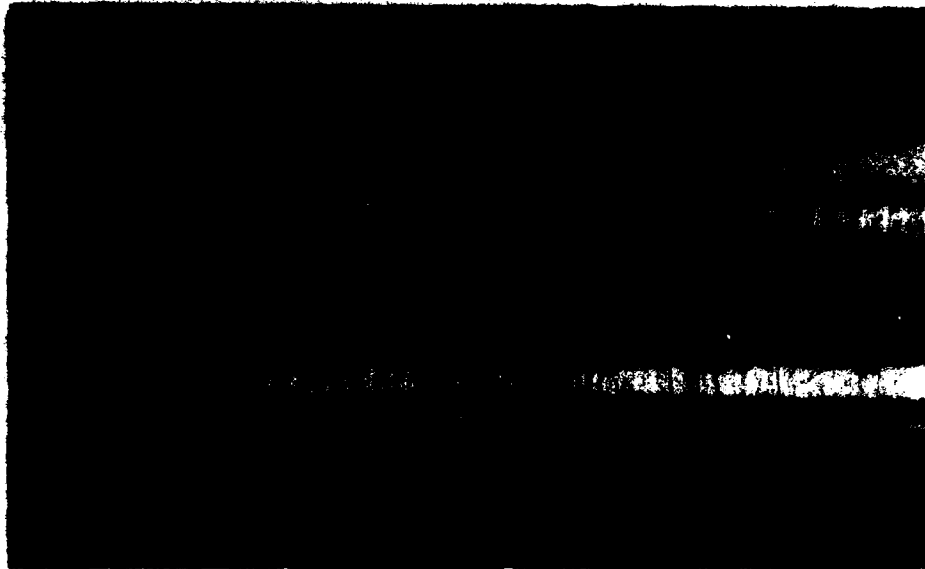


FIGURE 13  
Internal Surface of Test Section  
After 3 Months Exposure Test  
(3ppm copper injection)



FIGURE 12  
Internal Surface of Test Section  
After 3 Months Exposure Test  
(no copper injection)

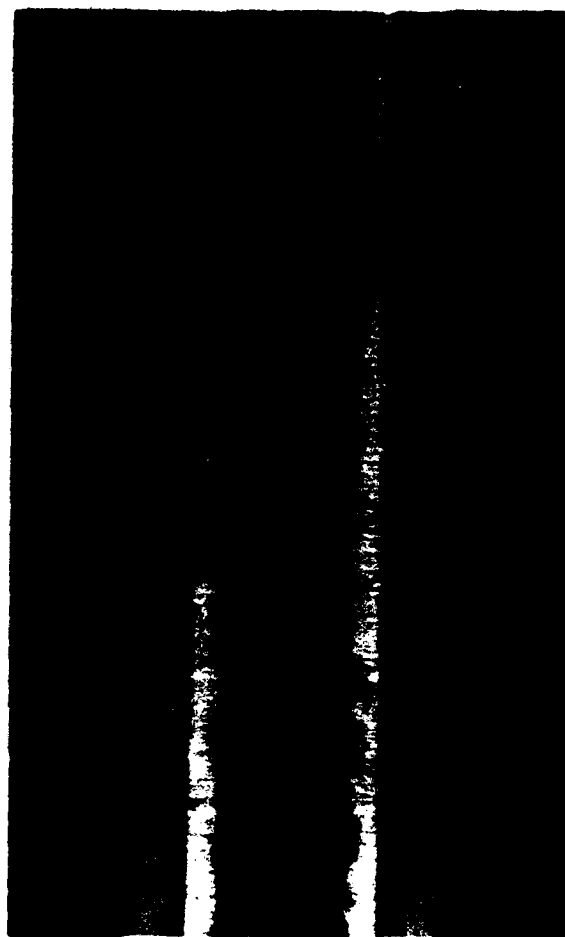


FIGURE 14 - Internal Surface of Coated Test  
Section After 3 Months Exposure Test  
(3ppm copper injection)

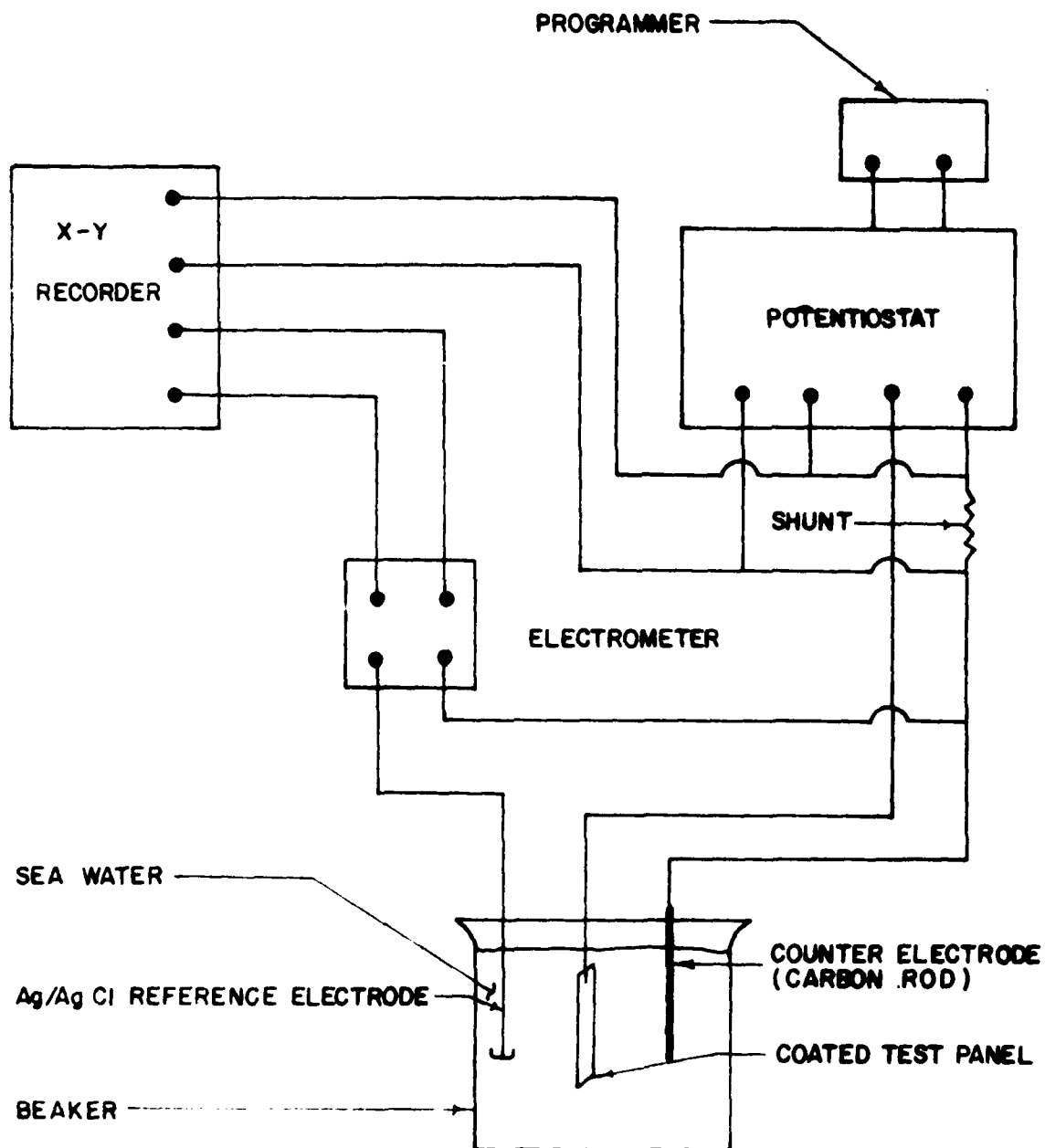


FIGURE 15 - TEST SET-UP FOR MAKING POLARIZATION MEASUREMENTS.

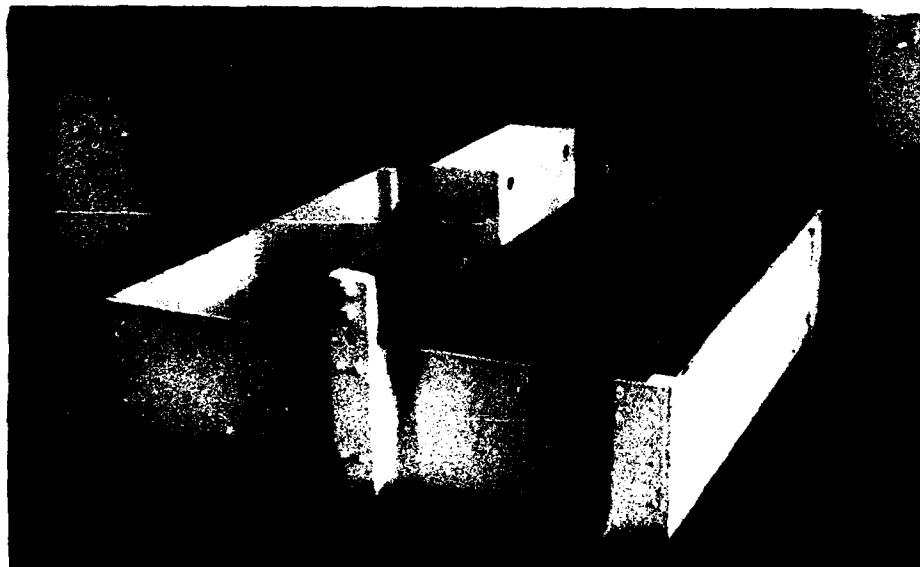
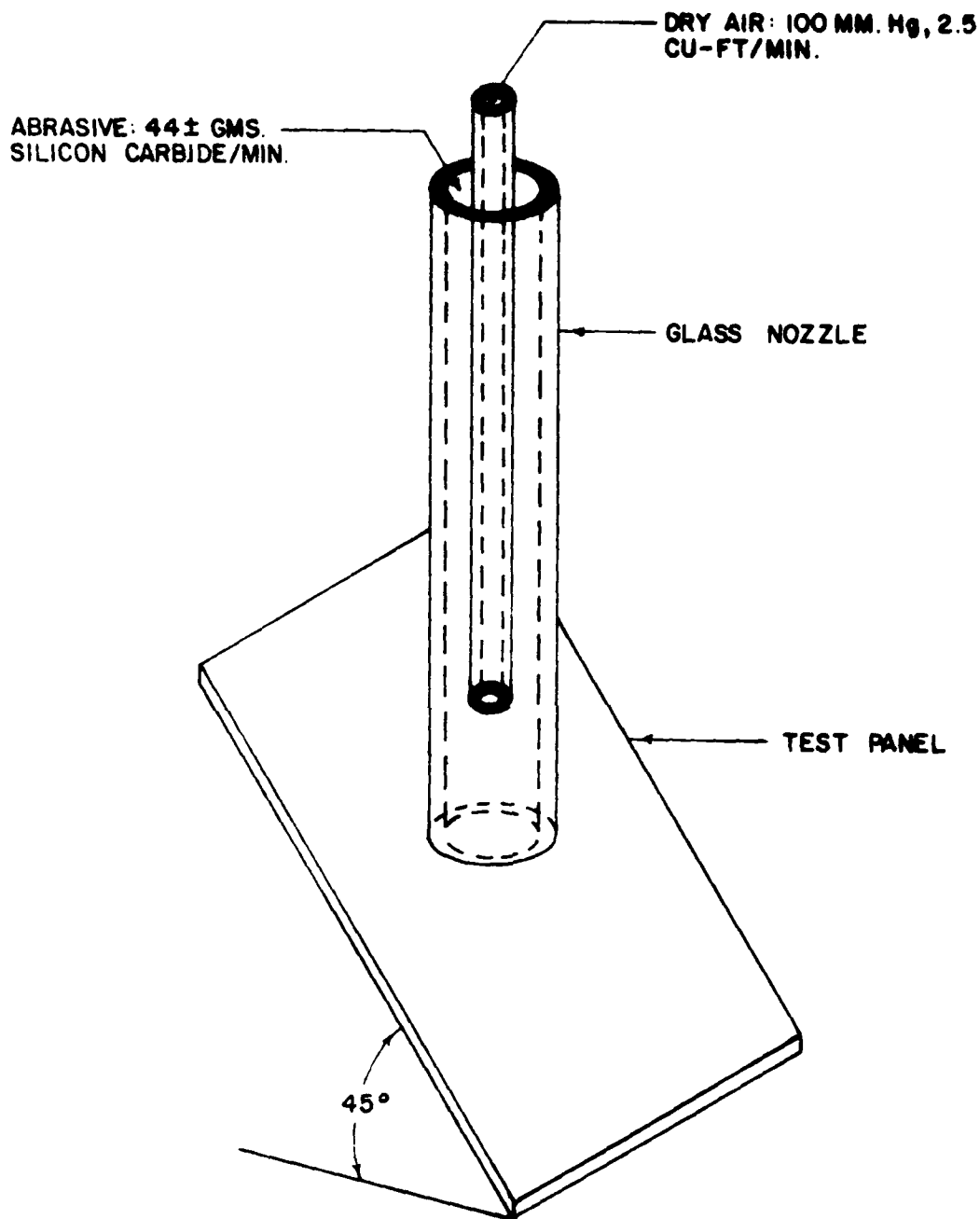


FIGURE 16 - Test Rig Built to Evaluate  
Non-Skid Deck Coatings



FIGURE 17 - Close-up of Test Rig Built to  
Evaluate Non-Skid Deck Coatings





$$\text{ABRASION COEFFICIENT} = \frac{\text{ABRASIVE USED, GMS}}{\text{COATING THICKNESS, MILS.}}$$

FIGURE 18 - SET-UP FOR ABRASION RESISTANCE TESTS.



FIGURE 19 - Nickel-Aluminide Coating (<15 mils)  
After 5 Month Exposure



FIGURE 20 - Nickel-Aluminide Coating (>15 mils)  
After 1 Month Exposure



FIGURE 21 - Nickel-Aluminide Coating (>15 mils)  
After 1 Month Exposure



FIGURE 22 - Wire-Spray Aluminum Coating  
After 1 Month Exposure

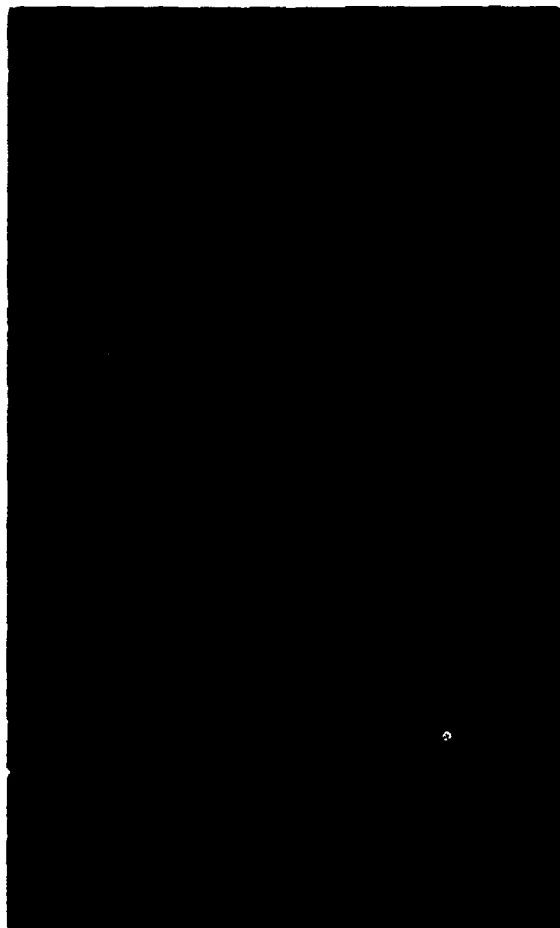
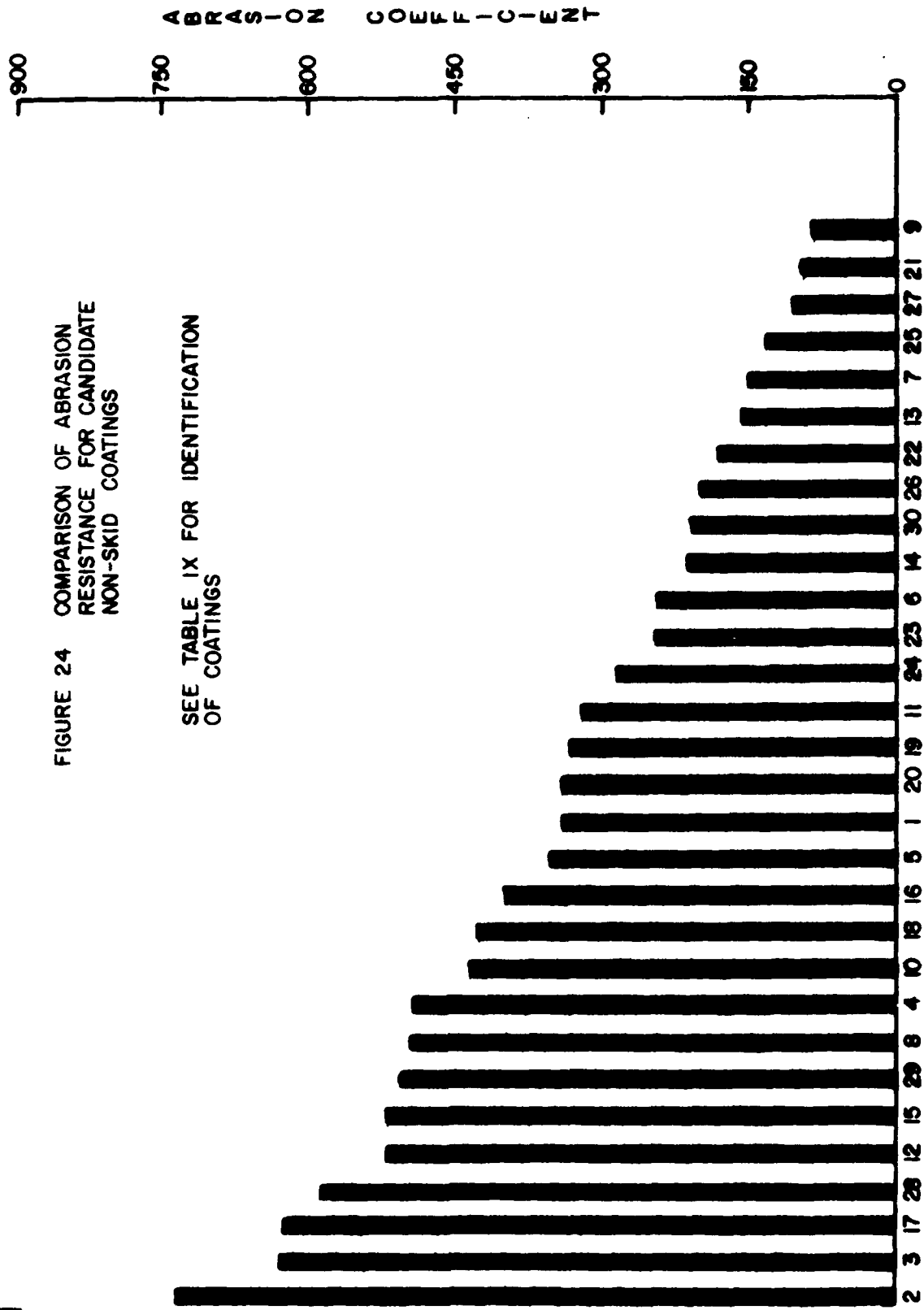


FIGURE 23 - Alumina-Titania Coating After  
9 Months Exposure



APPENDIX ITHE USE OF ELECTROCHEMICAL POLARIZATION TECHNIQUES  
TO MEASURE CORROSION RATES

Advances in electrochemistry in recent years have evolved test techniques that overcome some of the limitations of simple weight loss measurements. Several techniques utilizing electrochemical measurements are now available to determine the corrosion rate of a metal exposed to a corrosive electrolyte.

When a metal is in a state of reversible equilibrium with a solution of its ions, simultaneous oxidation and reduction reactions are taking place with no net change in the weight of the metal electrode or the concentration of ions. The rate of oxidation and reduction taking place can be expressed in terms of Faraday's Law:

$$(1) \quad r_{ox} = r_{red} = i_o/nF$$

where  $i_o$  is called the exchange current. Since oxidation current and reduction current have opposite polarities, at equilibrium there is no net current.

When the equilibrium of an electrode reaction is disturbed, there is a change in the potential of the electrode when measured against a stable reference. The difference between the equilibrium potential and the potential under the new conditions is called polarization and is usually designated by the Greek letter Eta,  $\eta$ . Mathematically:

$$(2) \quad \eta = E_{eq} - E$$

where  $E_{eq}$  is the potential at equilibrium and  $E$  is the potential under the new conditions. Disturbance of the equilibrium condition alters the exchange current balance and results in a net current flow, either oxidation or reduction, which is representative of the net rate of reaction. Polarization, therefore, results from any situation involving a net current flow to or from an electrode surface.

A metal undergoing corrosion involves two reactions, one at the cathode and one at the anode. Because of the current flow between local cathodes and anodes, a corroding metal polarizes toward a common potential,  $E_{cor}$ . The

behavior of the corroding metal is studied by application of an external current. A measured and externally controlled source of direct current is connected between the corroding metal and a counter electrode. The change in potential (polarization) of the corroding metal is then determined as a function of the externally applied current, either anodic or cathodic.

The polarization resistance technique for determining corrosion rates involves polarizing a test specimen + 20 millivolts from the corrosion potentials and measuring the currents associated with this partial polarization curve. Early researchers<sup>1</sup> thought that a linear relation existed between current and potential. They hypothesized that the slope of this "linear" polarization curve was inversely proportional to the corrosion rate according to the following expression:

$$(3) \frac{\Delta E}{\Delta I} = \frac{1}{2.3} \times \frac{\beta_a \times \beta_c}{\beta_a + \beta_c} \times \frac{1}{I_c}$$

where  $I_c$  = corrosion current density

$\beta_a$  = Anodic Tafel Slope

$\beta_c$  = Cathodic Tafel Slope

$\Delta I$  = Impressed Current Density

$\Delta E$  = Polarization caused by impressed current  
when  $\Delta E < 20$  millivolts

The corrosion rate is a linear function of  $I_c$  according to Faraday's Law:

$$\text{corrosion rate} = \frac{KI_c}{\rho}$$

where  $k$  = electrochemical equivalent for specific metal

$\rho$  = density of specific metal

Recent work by Mansfeld<sup>2</sup>, however demonstrates that there is no theoretical justification for polarization curves to be linear at or within + 20 millivolts of the corrosion potential. He shows, in fact, that non-linearity is severe in many cases. This does not void, however, this polarization technique for determining corrosion rates.

<sup>1</sup>M. Stern and A. L. Geary, "Electrochemical Polarization - Part 1, "Int. Electrochemical Soc., 104, (1957).

<sup>2</sup>F. Mansfeld, "Electrochemical Background of the Polarization Resistance Technique", a paper presented at the NACE Corrosion Conference, 1973.



Mansfield shows that with some modification of data analysis, polarization curves within  $\pm 20$  millivolts of the corrosion potential can still be used as a basis for accurately calculating corrosion rates. The modifications include determination of  $\frac{\Delta E}{\Delta I}$  @  $I = 0$  and application of curve fitting techniques to more precisely determine  $\beta_a$  and  $\beta_c$ . The formula hypothesized by Stern is then shown to be valid.

APPENDIX IIEVALUATION OF PROTECTIVE COATINGS BYELECTROCHEMICAL POTENTIAL AND POLARIZATION MEASUREMENTS

A semi-quantitative evaluation on the performance of protective coatings in many corrosive environments can be obtained from electrochemical potential and polarization measurements. These measurements are non-destructive and allow accurate direct calculation of corrosion rates for the coating/substrate in aqueous environments. The corrosion rate calculation proceeds according to the method described in Appendix I.

The basis for using calculated corrosion rates to evaluate coating performance can be seen by examining the characteristic manner in which a metallic, sacrificial-type coating behaves in an aqueous environment. If a metallic coating were applied perfectly to the substrate metal, it would be pore free and would corrode at a rate characteristic of the coated metal itself. However, no coating system can be considered pore free and, therefore, the calculated corrosion rate is a summation of both the local action corrosion rate for the coating metal and the galvanic corrosion rate caused by local bi-metal cells between substrate metal and coating metal. The number and intensity of localized bi-metal cells on the coated surface is a direct function of the porosity of the coating. Because the porosity of a metal coating increases as the metal corrodes or sacrifices, the corrosion reaction becomes self-stimulating. Polarization measurements allow calculation of the changing corrosion rate as a function of time. From the corrosion rate vs. time data, meaningful extrapolations can be made allowing prediction of the useful service life for individual coatings. This is not simply obtained by other methods.

For a non-metallic, barrier-type coating, the calculated corrosion rate indicates the amount of corrosion occurring at coating faults or "holidays" where the substrate metal is in contact with the environment. As the barrier-type coating deteriorates with time, the area of substrate metal exposed to environment will increase with a corresponding increase in corrosion. By comparing calculated corrosion rates versus time of exposure for different barrier coatings over a common substrate, the performance of the barrier coatings can be rated on a semi-quantitative basis. This type of data is usually much more discriminating than data compiled from visual inspection.

Electrical potential measurements also provide meaningful data for evaluating the performance of a metallic sacrificial-type coating. Initially, the substrate metal with a sacrificial-type coating would be expected to exhibit an electrochemical potential characteristic of the coating metal in the particular aqueous solution. As the metal coating sacrifices, the potential will change toward a value more characteristic of the substrate metal than the coating. Potential measurements with time will give a meaningful indication as to the performance of a sacrificial-type coating.

Although a typical environment is often more atmospheric than total immersion, polarization and potential measurements in sea water provide semi-quantitative performance data. The calculated corrosion rates in sea water are not, of course, identical in magnitude to the corrosion rates that will occur in the atmosphere. However, changes in the sea water corrosion rate or sea water potential as a function of time provide quantitative evidence of how a coating is performing in the atmosphere. These changes in the characteristic properties of the coating would not be obvious by physical inspection.

## APPENDIX III

FLEET EVALUATIONS OF VARIOUS NON-SKID  
COATINGS APPLIED TO JET BLAST DEFLECTORS

This appendix is a report of on-going sea evaluations of coatings selected prior to the laboratory tests discussed in this report. These coatings had been selected based on previous NAEC tests.<sup>3</sup>

<sup>3</sup> L. Moskowitz, "Development of Metallized Non-Skids for Jet Blast Deflectors" NAEC Report No. 7849, August, 1974.

<u>COATING**</u>	<u>CARRIER</u>	<u>MK7 JBD</u>	<u>TIME AT SEA</u>
1. Flame-Sprayed Nickel-Aluminide	CV-59	No. 1 (one module)	12 Months
3. Flame-Sprayed Nickel-Aluminide	CV-63	No. 1	30 Months
Flame-Sprayed Zinc	CVN-65	Nos. 1, 2, & 3	18 Months
Flame-Sprayed Nickel-Aluminide			
7. Arc-Sprayed Aluminum	CV-59	No. 1 (one module)	12 Months
	CV-67	Nos. 1 & 3 (half of each)	7 Months
10. Arc-Sprayed Aluminum-Molybdenum	CV-59	1 Module	1 Month
	CV-67	Nos. 1 & 3	7 Months
33. Flame-Sprayed Nickel-Aluminide	CV-63	No. 3	10 Months
	CV-67	Nos. 1 & 3	7 Months
	CVN-68	Nos. 1, 2, & 3	4 Months

\*\*Coating numbers were taken from Table IX

Coating No. 1 performed in the sea trials as predicted in the test program. Some pitting occurred, and in time spalling in small areas led to approximately 50 percent loss of coating after 13 months.

Coating No. 7 has performed well in the two carrier trials to date. When used on the No. 3 JBD, which is exposed to rubbing by the arresting cable, the modules on the CVA-67 have started to develop some smooth wear spots after seven (7) months; but they were still giving suitable non-skid performance.

Coating No. 3 has performed excellently in all of its carrier applications to date. It is the one coating which has been most exposed to the F-14 (on the CVAN-65). In the laboratory tests discussed in this report, the coating failed after only two (2) weeks of test. Unfortunately, the failure was obviously related to the manner in which jet blast and jet blast cooling was being simulated. This technique was changed after the failure of the sample coating, but the damage had already taken an irreversible toll; thus, the corrosion behavior of this coating was not evaluated in these tests.

Coating No. 10 looked good in both the Ocean City tests, as well as, tests run at NATF.<sup>3</sup> Yet after one (1) month of service in the CVA-59, serious spalling was observed to the extent that the module was removed from the carrier. Continued testing at NATF (where corrosion was not a factor) caused more spalling to occur. It would seem that while the corrosion behavior of this coating might be predicted by the Ocean City tests, the thermo-mechanical response to aircraft jet blasts was not accurately duplicated.

Coating No. 33 (MPR-1058) has performed erratically, doing well on the modules of the No. 3 JBD of the CV-63, CV-67 and CVN-68, but showing some blistering and delamination on the modules of the No. 1 and No. 2 JBD's of the CVN-68. Corrosion pits similar to those observed on an unsealed coating were also observed on some of the modules which had been exposed to the highest jet blast heat.

The corrosion behavior of this coating may well be explained by results obtained in the tests. The failure of the Metcoseal coating after jet blast exposure probably explains the corrosion pitting on some of the modules. The erratic blistering performance is very possibly a result of excessive coating thickness on some areas, again an effect predicted by the corrosion tests.

<sup>3</sup>L. Moskowitz, "Development of Metallized Non-Skids For Jet Blast Deflectors" NAEC Report No. 7849, August, 1974.

In reviewing the carrier evaluations vs the corrosion tests, it appears that the corrosion tests gave valuable insights into corrosion behavior of the various coatings; however, because of the failure to accurately simulate the thermo-mechanical effects of jet blasts, the tests cannot be used by themselves to predict JBD coating performance.